12-2009

Kinetic Studies of the Sulfoxidation of Aryl Methyl Sulfides by Trans-Dioxoruthenium(VI) Porphyrin Complexes

Chris Abebrese
Western Kentucky University, chris.abebrese@wku.edu

KINETIC STUDIES OF THE SULFOXIDATION OF ARYL METHYL SULFIDES BY TRANS-DIOXORUTHENIUM(VI) PORPHYRIN COMPLEXES

A Thesis

Presented to

The Faculty of the Department of Chemistry

Western Kentucky University

Bowling Green, Kentucky

In Partial Fulfillment

Of the Requirements for the Degree

Master of Science in Chemistry

By

Chris Abebrese

December 2009

KINETIC STUDIES OF THE SULFOXIDATION OF ARYL METHYL SULFIDES BY TRANS-DIOXORUTHENIUM(VI) PORPHYRIN COMPLEXES

Date Recommended December 7, 2009

Dr. Rui Zhang

Director of Thesis

Dr. Chad Snyder

Dr. Cathleen Webb

Dean, Graduate Studies and Research Date

ACKNOWLEDGEMENT

It is a pleasure to show my appreciation and acknowledge all the noble people who made this thesis possible. First and foremost, I owe my deepest gratitude to my research advisor, Dr. Rui Zhang, whose encouragement, guidance, and support from the beginning to the end of the project enabled me to develop an understanding of the subject. This thesis would not have been possible without his ingenuity and for that I am indebted to him.

It is of great honor to have Dr. Cathleen Webb and Dr. Chad Snyder to serve on my thesis committee. Their suggestions and various contributions were very helpful and cannot be overlooked. I would like to also show my gratitude to members of my research group, Huang Yan, Wesley Cartwright, and Eric Vanover; for their support and many contributions towards this project. This project would have been unbearable without their help, so I wish them all the best in their various endeavors.

Last, but not the least, I am sincerely indebted to my family, especially my brother Nelson Abebrese, for the unconditional support and tolerance shown to me throughout the course of my study.

I dedicate this thesis to my parents especially in loving memory of my late father, Mr. David Awuah Abebrese, may his soul rest in perfect peace.

TO GOD BE THE GLORY!!!!

TABLE OF CONTENTS

LIST OF TABLES

LIST OF FIGURES

LIST OF SCHEMES

ABBREVIATIONS AND SYMBOLS

ArH	Aryl Hydrogen
β-H	Pyrrolic Hydrogen
CYP450	Cytochrome P-450
$CYP450_{cam}$	Cytochrome $P\text{-}450_{cam}$
FT-IR	Fourier-Transform Infrared
FT-NMR	Fourier-Transform Nuclear Magnetic Resonance
H_2TPP	*meso*-Tetraphenylporphyrin
H_2TPFPP	*meso*-Tetrakis(5,10,15,20-pentafluorophenyl)porphyrin
k_2	Second-order rate constant
k_{obs}	Observed pseudo-first-order rate constant
m-CPBA	*meta*-Chloroperoxybenzoic acid
NADH	Nicotinamide adenine dinucleotide
NADPH	Nicotinamide adenine dinucleotide phosphate
PhIO	Iodosylbenzene
$[Ru^{II}(CO)TPP]$	Carbonyl(5,10,15,20-tetraphenylporphyrinato) Ruthenium(II)
$[Ru^{II}(CO)TPFPP]$	Carbonyl[5,10,15,20tetrakis(pentafluorophenyl)porphyrinato] Ruthenium(II)
$[Ru^{VI}(O)_2TPP]$	*trans*-Dioxo(5,10,15,20-tetraphenylporphyrinato) Ruthenium(VI)
$[Ru^{VI}(O)_2TPFPP]$	*trans*-Dioxo[5,10,15,20-tetrakis(pentafluorophenyl)porphyrinato] Ruthenium(VI)
TMP	*meso*-tetrakis(2,4,6-trimethylphenyl)porphyrinato
UV-vis	Ultraviolet-visible

KINETIC STUDIES OF THE SULFOXIDATION OF ARYL METHYL SULFIDES BY TRANS-DIOXORUTHENIUM(VI) PORPHYRIN COMPLEXES

Chris Abebrese December 2009 65 Pages

Directed by: Dr. Rui Zhang

Chemistry Department Western Kentucky University

ABSTRACT

The development of an efficient, catalytically active, biomimetic model for cytochrome P-450 enzymes has been an area of intense research activity. Ruthenium porphyrin complexes have been the center of this research and have successfully been utilized, as catalysts, in major oxidation reactions such as the hydroxylation of alkanes, the epoxidation of alkenes and aromatic rings, and the N-oxidation of amines, among others. In this project, the kinetics of two-electron sulfoxidation of *para*-substituted phenyl methyl sulfides to the corresponding sulfoxides with well-characterized *trans*-dioxoruthenium(VI) porphyrin complexes were studied by rapid stopped-flow spectroscopy. The substituent effect in sulfides and in dioxoruthenium(VI) complexes were also kinetically investigated.

The low-reactive *trans*-dioxoruthenium(VI) porphyrin complexes (**3a-b**) were synthesized from the oxidation of their carbonylruthenium(II) porphyrin precursors with *m*-chloroperoxybenzoic acid (*m*-CPBA) and characterized spectroscopically by ^{1}H-NMR, IR, and UV-vis. The low-reactivity of these complexes makes them suitable for kinetic studies. The sulfoxidation with the *trans*-dioxoruthenium(VI) species followed a pseudo-first order kinetic decay from Ru^{VI} to Ru^{IV} species with no accumulation of

intermediates. The reactivity order in the series of dioxoruthenium(VI) complexes follows **3b** > **3a** >**3c**, which is consistent with expectations based on the electrophilic nature of high-valent metal-oxo species. Steric effect of the substituents on the complexes also affected the reactivity order. The kinetic results revealed that the sulfoxidation reaction with these well-characterized dioxoruthenium(VI) complexes is 3 – 4 orders of magnitude faster than the epoxidation reaction with the same complexes under similar conditions.

I. INTRODUCTION

1.1. General

Oxidation reactions are of fundamental importance in Nature, and are key transformations in organic synthesis.[1] Traditionally, oxidative transformations have been achieved with stoichiometric amounts of inorganic oxidants, notably chromium(VI) reagents, which generate large amounts of toxic inorganic by-products and are often conducted in environmentally undesirable conditions.[2-4] Today there is an increasing demand for the utilization of clean and environmentally friendly oxygen sources such as dioxygen, hydrogen peroxide, and alkyl hydroperoxides for selective oxidation because these oxygen sources are atom efficient and produce water as the by-product.[1-5] However, due to the high energy barrier associated with the electron transfer between the organic substrate and atmospheric oxygen, direct oxidation of organic substrates by either dioxygen or hydrogen peroxide is kinetically unfavorable.[1] Consequently, the development of catalytic oxidation methods that use dioxygen or hydrogen peroxide as the stoichiometric oxygen donor, is one of the most important goals in oxidation chemistry.[2] Catalytic oxidation plays an important role in the production of commodity chemicals.[5]

In biological systems, catalytic oxidations facilitated by oxidative enzymes are fundamental in many biosynthesis and biodegradation processes.[5,6] Most of these biological oxidations are mediated by heme-containing oxygenases. The most prominent of these oxygenases is the ubiquitous cytochrome P-450 monooxygenase (CYP450). The CYP450 enzymes have been shown to effect a vast range of oxidation reactions in Nature, which include important transformations such as alkene epoxidation and alkane

hydroxylation, many of which are characterized by high degrees of chemo-, regio-, and enantioselectivities.[5-7] The most common heme prosthetic group found in heme-containing enzymes is the iron protoporphyrin IX (heme *b*) complex (Figure 1),[8] which is reported as the active site of the heme enzymes.[5]

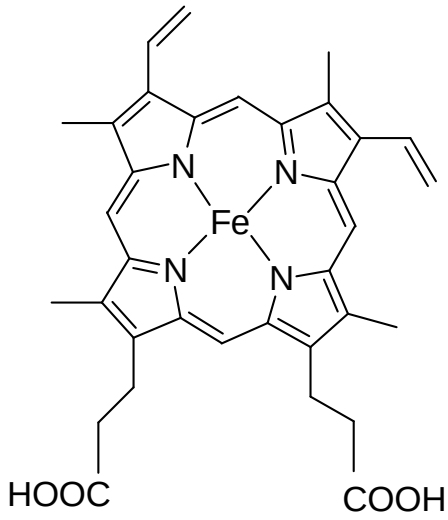

Figure 1. Structure of iron protoporphyrin IX (Heme *b*)

As a result of the unique spectral properties as well as the efficiency of the cytochrome P-450 enzymes to catalyze a variety of difficult biotransformations,[6] significant efforts have been directed toward creating artificial mimics of these remarkable enzymes.[4] Effective catalytic systems for the selective oxidation (Scheme 1) based on metalloporphyrins with iron, manganese, and ruthenium transition metals have been synthesized as biomimetic models of the CYP450 enzymes.[4,9] In the past decades, many synthetic metalloporphyrin complexes have been reported to reproduce and mimic a variety of the heme-enzyme mediated reactions (Scheme 1).[10] This research was

stimulated by the desire for better understanding of the intricate mechanisms of biochemical pathways using simple biomemitic models.[5]

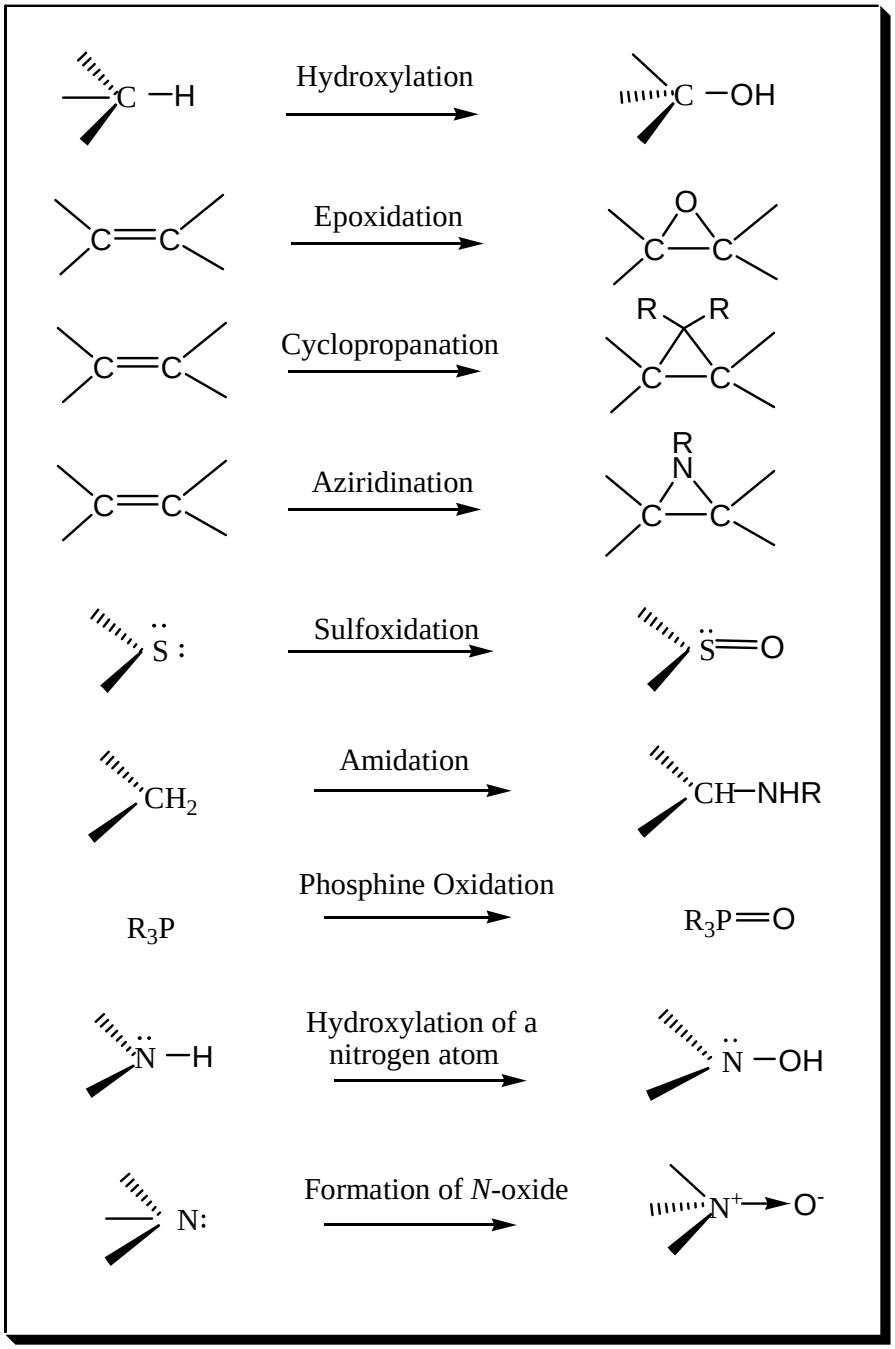

Scheme 1. Typical metalloporphyrin-mediated reactions

In this thesis, a set of ruthenium porphyrin complexes have been synthesized and spectroscopically characterized based on literature knowledge. Kinetic studies of sulfide oxidations (sulfoxidations) by the low-reactive and well-characterized *trans*-dioxoruthenium(VI) porphyrin complexes have been conducted using the rapid stopped-flow technique. The kinetic results have also been compared to the well known kinetics of alkene epoxidation.

1.2. Overview of Cytochrome P-450 Enzymes (CYP450)

Early works by Hayaishi et al. led to the discovery of an enzyme that was able to incorporate atmospheric dioxygen into organic substrates, and these enzymes were designated as oxygenases.[8] Oxygenases can incorporate one oxygen atom (monooxygenases) or both oxygen atoms (dioxygenases) from dioxygen into an organic substrate. It is known that oxygenases are present in all living forms including animals, plants, and microorganism.[8] Enzyme-catalyzed oxidations received a lot of attention following the discovery of oxygenases. Further studies by Omura and Sato identified a heme protein containing protoheme IX (Figure 1), based on earlier studies by Garfinkel et al. who first discovered the presence of the pigment in liver microsomes.[8] This pigment was later assigned the name cytochrome P-450 because of the characteristic Soret absorption band at a wavelength of 450 nm observed for the ferrous-carbonyl complex.

To date over 8100 distinct cytochrome P-450 genomes are known to exist, but few have been studied in detail.[11] The CYP450 enzymes are extensively distributed in Nature. They have been isolated in numerous mammalian tissues (eg. liver, kidney, lung, intestine, adrenal cortex), as well as in plants, bacteria, fungi, insects, and so on.[4,8] Cytochrome P-450 enzymes are a superfamily of heme-thiolate proteins known to perform two main functional roles in biological systems. The first is the metabolism of xenobiotics (compounds exogeneous to the organism) as a protective role of degradation or solubilization of molecules in preparation for excretion. The second is the biosynthesis of critical signaling molecules used for control of development and homeostasis.[6] In mammalian tissues these roles are accomplished via the metabolism of drugs and xenobiotics, the synthesis of steroid hormones, the metabolism of fat-soluble vitamin, and

the conversion of polyunsaturated fatty acids to biologically active molecules.[6] However, cytochrome P-450 enzymes can convert certain unreactive xenobiotics to highly reactive, electrophilic metabolites which can mutate DNA[8] and induce carcinogenesis.

Cytochrome P-450 enzymes are classified as monooxygenases (Scheme 2). Thus they are able to incorporate one oxygen atom from atmospheric dioxygen into a substrate and reduce the second oxygen to water, utilizing reducing agents such as NADH (nicotinamide adenine dinucleotide) or NADPH (nicotinamide adenine dinucleotide phosphate) as electron donor via electron transport protein systems.[8]

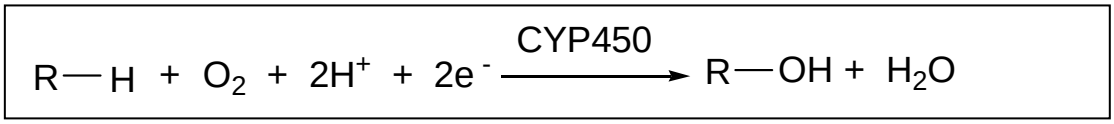

Scheme 2. Monooxygenase reaction

The R in Scheme 2 represents a variety of organic substrates, normally non-polar aromatic or aliphatic molecules,[12] catalyzed by the CYP450 enzymes.

The majority of the CYP450 enzymes are membrane-bound usually found in the inner mitochondrial and the endoplasmic reticulum of microsomal membranes.[8] The structurally and biochemically best-characterized cytochrome P-450 is the soluble camphor-inductible bacterial CYP450 monooxygenase ($CYP450_{cam}$), which was first identified in *Pseudomonas putida*.[8,13] The soluble bacterial $CYP450_{cam}$ (Figure 2) are very stable, making them easier to express and to purify in large quantities.[11] As reported in the literature, recent crystallographic structures of mammalian CYP450 reveals that the overall structural fold of the eukaryotic membrane bound CYP450 clearly resembles that

of the soluble bacterial $CYP450_{cam}$.[15] Thus $CYP450_{cam}$ remains a useful model system for the structural and functional studies of cytochrome P-450 enzymes.

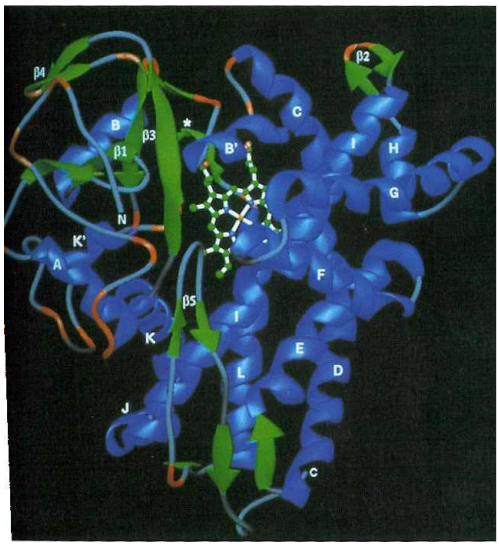

Figure 2. X-ray structure of cytochrome $P\text{-}450_{cam}$

Cytochrome $P450_{cam}$ catalyzes the regio- and stereospecific 5-*exo* hydroxylation of the bicyclic terpene camphor with molecular oxygen to 5-*exo*-hydroxycamphor[13-14] (Scheme 3),[8] providing insight into the catalytic cycle of cytochrome P450 enzymes (Scheme 4).

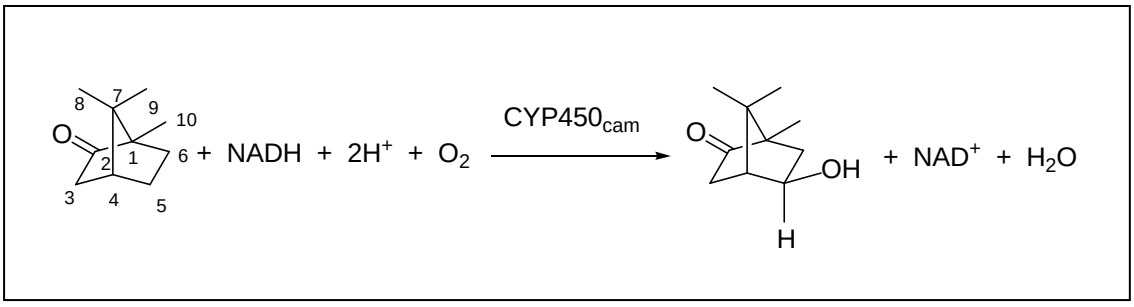

Scheme 3. Stereoselective hydroxylation catalyzed by $CYP450_{cam}$

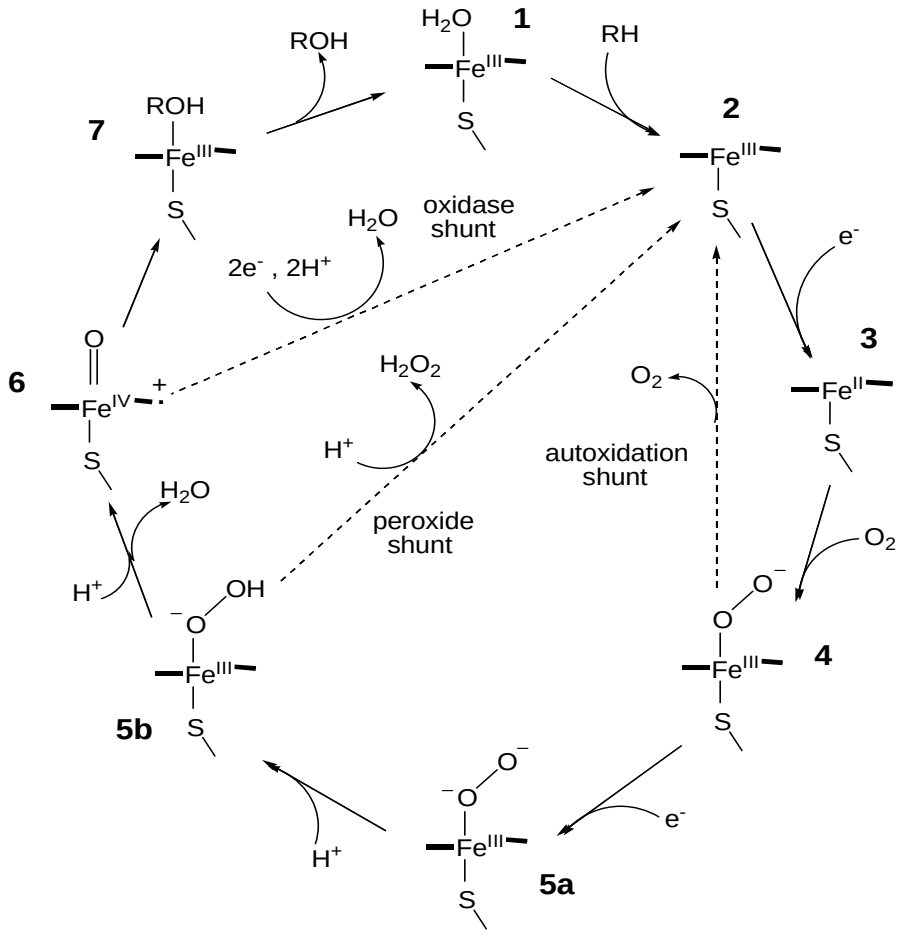

Scheme 4. Catalytic cycle of cytochrome P-450

The catalytic cycle of CYP450 including postulated structures of putative intermediates, as reported in literature, is shown above (Scheme 4).[6,8] The RH represents the substrate and ROH represents the corresponding product. State **6** is a hypothetical intermediate whose structure has not been established. Structures **1**, **2**, and **6** are neutral, while the overall charge on **3**, **4**, and **5b** is -1 and on intermediate **5a** is -2. The radical state of intermediate **6** indicates the electron deficiency of the π-electron system of the

porphyrin ring.[8] As documented in the literature, the cytochrome P-450 reaction cycle involves four well-characterized and isolable states [8] (**1** – **4** in Scheme 4). Substrate binding to the six-coordinate low-spin ferric resting state of the enzyme (**1**) perturbs the water coordinated as the sixth ligand of the heme iron, and generates the five-coordinate high-spin ferric state (**2**). The change in spin states from low to high, significantly increases the redox potential of the enzyme's heme.[8] Thus, the high-spin intermediate **2** has a more positive reduction potential,[6] making it easier to reduce to the five-coordinate high-spin ferrous state (**3**).[6,8] Oxygen binding to the ferrous state forms the oxyferrous complex (**4**), which is the last relatively stable intermediate in this cycle.[6] The reduction of this complex, the rate limiting step in the cycle,[8] is proposed to yield a peroxy-ferric intermediate (**5a**), which can be protonated to form the hydroperoxide intermediate (**5b**). A second protonation at the distal oxygen atom leads to heterolytic O – O bond cleavage releasing water and generating the proposed oxo-ferryl porphyrin radical intermediate **6**, which is equivalent to the high-valent iron(V)-oxo intermediate of peroxidase enzymes.[6] The cycle is completed when intermediate **6** oxygenate the substrate to form the product complex (**7**) and then regenerate intermediate **1**.[6,8] The CYP450 reaction cycle also contains at least three branch points, where multiple side reactions are possible and often occur under physiological conditions.[6] According to Denisov and co-workers, the three major abortive reactions are (i) autoxidation of the oxy-ferrous intermediate (**4**) with concomitant production of a superoxide anion and return of the enzyme to intermediate **2**, (ii) a peroxide shunt, where the coordinated peroxide or hydroperoxide anion (**5a,b**) dissociates from the iron forming hydrogen peroxide, thus completing the unproductive (in terms of turnover) two-electron reduction of oxygen, and (iii) an oxidase uncoupling

wherein the ferryl-oxo intermediate (**6**) is oxidized to water instead of oxygenation of the substrate, which results effectively in four-electron reduction of two molecules of water.[6]

The true oxidant in cytochrome P-450 enzymes have not been observed under natural conditions; however, it is usually thought to be an iron(IV) – oxo porphyrin radical cation (intermediate **6)**, which is traditionally referred to as Compound I.[16] As illustrated in Scheme 4, the oxidants in CYP450 are formed by a sequence of reductions, oxygen binding, and protonation steps. Analogues of Compound I in the model system are relatively low reactivity oxidizing species.[16] Compound I of chloroperoxidase from *Caldariomyces fumago* is the best available model for the putative Compound I in CYP450, and it is reported to catalyze two-electron, oxo-transfer oxidation reactions that mimic those catalyzed by CYP450 enzymes.[16] Newcomb and co-workers conducted a kinetic study of two-electron oxidations by Compound I derivative of chloroperoxidase, and deduced that the rate constants for the chloroperoxidase Compound I oxidation reactions are 2-3 orders of magnitude greater than those of model compounds.[16]

1.3. Biomimetic Models of Cytochrome P-450 Enzymes

The development of new processes that employ transition metals as substrate-selective catalysts and stoichiometric environmentally friendly oxygen donors, such as molecular oxygen or hydrogen peroxide, is one of the most important goals in oxidation chemistry.[1] Nonetheless, direct oxidation by molecular oxygen or hydrogen peroxide is kinetically unfavorable due to the triplet ground state of dioxygen. One way to overcome the high kinetic barrier inherent to the reaction of triplet O_2 is to utilize transition metals, which in the appropriate oxidation state, can form dioxygen adducts with triplet O_2, and, thus, are capable of undergoing monooxgenase reactions with organic substrates.[8] Consequently, considerable efforts have been directed to the synthesis of biomimetic transition metal catalysts for stereo- and regioselective organic oxidations.[17]

Many metalloporphyrin complexes have been synthesized as biomimetic models of cytochrome P-450 with the aim of developing enzyme-like catalysts, and probing the mechanisms of biological processes. An extensive variety of metalloporphyrin complexes using transition metals such as iron, manganese, chromium, and ruthenium have been developed to mimic and understand the activities of cytochrome P-450 enzymes. Nature selected iron protoporphyrin IX to mediate intrinsically difficult oxidations with dioxygen at the heme center of cytochrome P-450 monooxygenases.[18] Groves et al first reported a simple iron porphyrin system as a CYP450 model that catalyzed the effective stereospecific alkene epoxidation and alkane hydroxylation in 1979 (Scheme 5).[4] This model system introduced the use of iodosylbenzene as an oxygen transfer agent to mimic

the chemistry of CYP450. High-valent oxoironporphyrin complexes were later discovered as the reactive intermediates in the iron porphyrin model systems.[4]

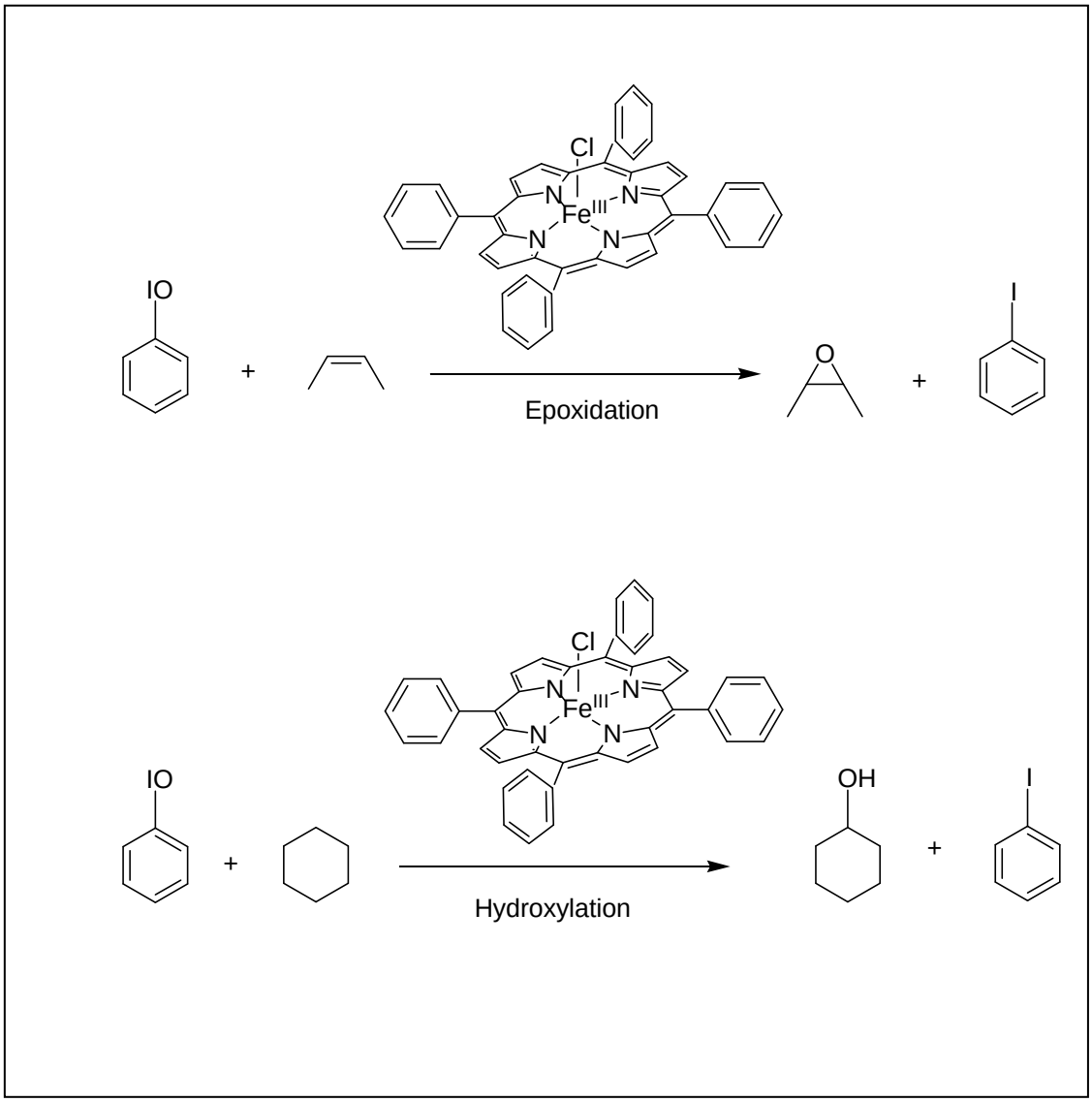

Scheme 5. Alkene epoxidation and alkane hydroxylation catalyzed by iron porphyrin system, Fe^{III}(TPP)Cl.

1.3.1. High-Valent Transition Metal-Oxo Species

The study of high-valent metalloporphyrins as models for the ubiquitous cytochrome P-450 enzymes has been receiving current attention.[19] An oxoiron(IV) porphyrin cation radical species is suggested to be the reactive intermediate in the oxygen atom transfer of reactions of monooxygenase enzymes.[4,19] There have been several reports on the chemistry of iron(IV) porphyrins in the last decade; however, the intrinsic reactivity and liability of high-valent iron-oxo complexes hamper detailed mechanistic studies on their oxidation chemistry.[19] In view of this, there have been growing interest in substituting iron with other metals[19] such as manganese and ruthenium.

Ruthenium porphyrins and related complexes have received considerable attention because of the close periodic relationship to iron, and the rich coordination and redox chemistry of ruthenium, which spans oxidation states from +2 to +7 in the porphyrin ligand environment.[18] Ruthenium complexes have a variety of useful characteristics including high electron transfer ability, high Lewis acidity, low redox potentials, and stability of reactive metal species such as oxo-metal, metallacycles, and metal carbene complex.[5] Ruthenium porphyrins have been shown to catalyze aerobic epoxidation of olefins under mild conditions and promising reactivity with nitrous oxide.[4,9] Studies show that high-valent ruthenium-oxo complexes in various oxidation states and with tunable physical and chemical properties can be isolated using a variety of macrocyclic ligands.[5] The mechanism of aerobic epoxidation mediated by ruthenium porphyrins (Scheme 6) has been examined , and a *trans*-dioxoruthenium(VI) complex was found to be the active oxidant.[18] It has been well established that *trans*-

dioxoruthenium(VI) porphyrins are potent oxidants for alkenes and alkanes.[17] The *trans*-dioxoruthenium(VI) porphyrin complexes are neutral, readily dissolve in nonpolar organic solvents, and are reactive toward alkene epoxidations and alkane hydroxyalations.[5] Moreover, they can be modified to form highly reactive chiral metal-oxo reagents, thus providing a unique opportunity to probe and understand the mechanism of metal-mediated asymmetric oxidations.[5] As reported by Groves et al. and depicted in Scheme 6, *trans*-dioxoruthenium(VI) porphyrin reacts with alkenes to form 1 equivalent of epoxide and 1 equivalent of Ru(IV)-oxo species. Two Ru(IV)-oxo molecules disproportionate to give the *trans*-dioxoruthenium(VI) species and Ru(II) porphyrin. The Ru(II) species is in turn oxidized by dioxygen into Ru(IV)-oxo complex closing the catalytic cycle.[4]

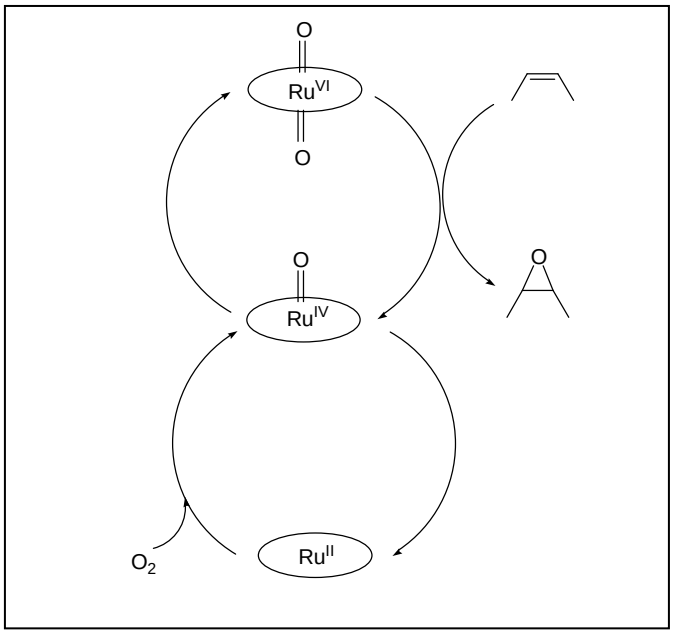

Scheme 6. Catalytic cycle of aerobic epoxidation of alkenes with *trans*-dioxoruthenium(VI) porphyrin complex

1.4. Sulfoxidation Reactions

The oxidation of sulfides to sulfoxides is of significant importance in organic chemistry.[20] Organic sulfoxides are valuable synthetic intermediates for the production of a variety of chemically and biologically active molecules, including therapeutic agents such as anti-ulcer (proton pump inhibitors), antibacterial, antifungal, anti-atherosclerotic, antihypertensive and cardiotonic agents, as well as psychotonics and vasodilators.[21,22] Organic sulfoxides are also versatile synthons for C-C bond formation, molecular rearrangements, and functional group transformations.[20,23] Selective oxidation of organic sulfides is very important from both industrial and green chemistry points of view because organosulfur compounds are a major source of environmental pollution.[23]

In view of the importance of sulfoxides, a number of methods have been developed for the oxidation of sulfides to the corresponding sulfoxides, since the first report by Marcker in 1865.[20] A variety of reagents have been utilized for this key transformation; however, many of them are either harmful or expensive, or cause over-oxidation to sulfones.[20-23] Surendra et al. reported the selective oxidation of sulfides to sulfoxides with *N*-bromosuccinimide in the presence of β-cyclodextrin in water under mild conditions without over-oxidation to sulfones.[23] Kowalski et al. also reported halogen-mediated oxidation of sulfides to sulfoxides under various conditions.[20] There have also been some kinetic studies on transition metal catalyzed sulfide oxidations. Chellamani and co-workers reported the kinetics and mechanism of (salen)Mn^{III} catalyzed hydrogen peroxide oxidation of alkyl aryl sulfides and proposed a

mechanism supported by electronic-oxidant and electronic-substrate effect studies, involving a manganese(III)-hydroperoxide complex as reactive species.[24]

A number of new methods for sulfoxidation reactions with hydrogen peroxide (H_2O_2) and catalyzed by transition metal complexes have been developed and reported.[22] Apparently, many of these transition metal catalysts show good catalytic properties, non-toxicity, safety in storage and operation, and air stability.[22] Whilst the oxidation of sulfides to sulfoxides catalyzed by transition metal complexes using clean and safe oxygen source such as hydrogen peroxide has been reported,[21,22] sulfoxidation reactions catalyzed by oxoruthenium species has received less attention. Despite the advancement in the development of this transformation, the exact mechanism for sulfoxidation reactions are still less understood.[21]

Recently, studies of metal complexes-catalyzed oxidations of alkenes, alkanes, and sulfides by dioxygen or peroxides are being given considerable attention in view of their relevance in understanding the mechanism of biological processes.[24] Extensive studies on the epoxidation and hydroxylation of hydrocarbons by metal-oxo species to the corresponding epoxides and alcohols, respectively, are well established in the scientific literature. There have been several reports on *trans*-dioxoruthenium(VI) porphyrin catalyzed hydrocarbon oxidation reactions, following the characterization of the first *trans*-dioxoruthenium(VI) porphyrin complex in the early 80s by Groves and co-workers.[4,19] For instance, Che et al. published a paper on the synthesis, spectroscopy, and reactivities of high-valent ruthenium(IV) and –(VI) oxo complexes of

octaethylporphyrin.[19] However, studies on sulfoxidation reactions by the well-characterized *trans*-dioxoruthenium(VI) porphyrin complexes are not reported yet.

II. EXPERIMENTAL SECTION

2.1. Materials & Chemicals

Commercially available *para*-substituted aryl methyl sulfides such as 4-methoxy thioanisole, methyl *p*-tolyl sulfide, 4-fluorothioanisole, 4-chlorothioanisole, and thioanisole were obtained from Alfa Aesar, and used as received for the kinetic studies. All the solvents for the synthesis are of analytical grade and used without further purification. The pyrrole was purchased from Sigma Aldrich and was freshly distilled before use. Bottles of benzaldehyde, propanoic acid, *cis*-cyclooctene, triruthenium dodecacarbonyl, *meta*-chloroperoxybenzoic acid (*m*-CPBA), $H_2(F_{20}$-tpp) (synthetic grade), aluminum oxide, pyrazole, chloroform-d, and Decalin (decahydronaphthalene) were purchased from Sigma Aldrich and also used as received.

2.2. Methods & Procedures

2.2.1. Physical Measurements

UV-visible spectra were recorded on an Agilent 8453 diode array spectrophotometer (Figure 3-4). Infra-red (IR) spectra were obtained as KBr disc on a Perkin Elmer Spectrum One FT-IR Spectrometer. ^{1}H NMR spectra were recorded on a JEOL 500 FT-NMR.

2.2.2. Distillation of Pyrrole

The purchased pyrrole was distilled before used. About 25 mL pyrrole was added to a 50 mL round-bottom flask containing a magnetic spin vane equipped with a

distillation apparatus. The pyrrole was distilled at 130^{o}C. The first distillate before 130^{o}C was discarded. The freshly distilled pyrrole was collected and immediately used for the synthesis of the free porphyrin ligand.

2.2.3. Stoichiometry and Product Analysis

The stoichiometric oxidation of thioanisole by different *trans*-dioxoruthenium(VI) complexes was studied. A solution of a *trans*-dioxoruthenium(VI) complex (1.0 mM) was added to thioanisole (0.2 M) in chloroform. A few drops of diphenylmethane were added as internal standard. The reaction mixture was stirred overnight under room temperature (22 ± 2^{o}C). The reaction yielded sulfoxide as the only detectable organic product by ^{1}H-NMR, δ = 2.7 ppm, as seen from the methyl signal.

2.2.4. Kinetic Measurements

Kinetic Measurements were conducted using Agilent 8453 diode array spectrophotometer coupled with Pro-K 2000 Rapid Kinetic System (Figure 3-4). A standard 1.0 cm quartz cuvette was used for the epoxidation kinetics, whereas the rapid stopped-flow system (Figure 4) was used for the *fast* sulfoxidation kinetic studies. This system uses a rapid mixing technique that can detect the reaction progress as short as 100 miniseconds. It also ensures equal mixing of the substrate and complex at the same time. Kinetics was studied by monitoring the decay of the Soret absorption band of the metal-oxo species at room temperature. A solution of dioxoruthenium(VI) porphyrin in chloroform or dichloromethane was treated with at least 100-fold excess of the substrate, *cis*-cyclooctene or *para*-substituted sulfide for the epoxidation and sulfoxidation

reactions respectively. A small percentage of pyrazole (2% w/w) was used for the epoxidation kinetic studies.

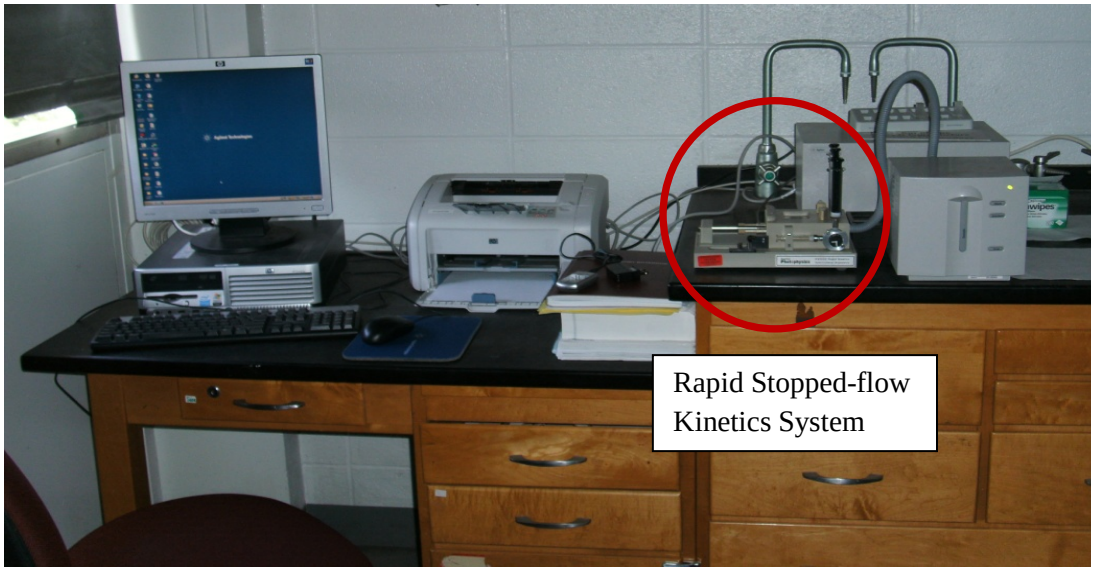

Figure 3. Agilent 8453 diode array spectrophotometer

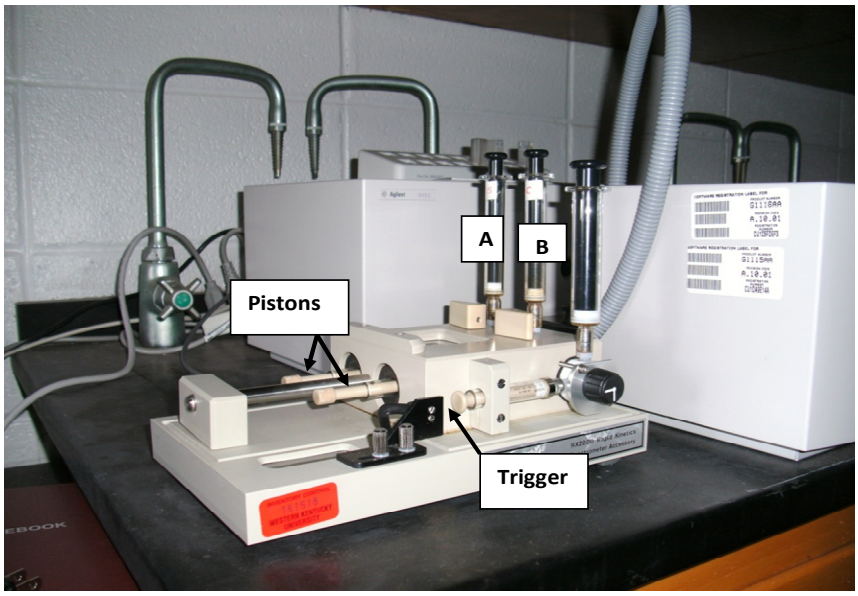

Figure 4. Pro-K 2000 rapid kinetics system

The absorbance *(A)* of the Soret band in the UV-visible spectrum of the reaction mixture at different reaction time *(t)* was measured. The pseudo-first order rate constants *(k_{obs})* were obtained by a nonlinear least-squares fit of *($A_f - A_t$)* to time *(t)* over four half-lives *($t_{1/2}$)* according to the following equation:

$$(A_f - A_t) = (A_f - A_i)\exp(-k_{obs}t)$$

Where A_f and A_i are the final and initial absorbance, respectively, and A_t is the absorbance measured at time *t*. Upon knowing the k_{obs} values at various reaction concentrations of the substrate, the second order rate constants (k_2) were determined as the slope from the linear least-squares fitting of the k_{obs} values versus substrate concentration plot.

2.3. Synthesis and Spectroscopic Characterization of Ruthenium Porphyrin Complexes

2.3.1. Synthesis and Characterization of *meso*-Tetraphenylporphyrin (H_2TPP) (1a)

The free porphyrin ligand was synthesized according to the known literature method developed by Adler et al.[25] The reaction for the synthesis of H_2TPP (**1a**) is shown in Scheme 7. Freshly distilled pyrrole (5 mL, 72 mmol) and benzaldehyde (7 mL, 69 mmol) are added to 30 mL solution of reagent-grade propanoic acid. After refluxing for 30 minutes at 120^{o}C, the solution is cooled to room temperature and then subjected to vacuum filtration to collect the solid precipitate. The filter cake is washed thoroughly with methanol until the filtrate is colorless. The resulting deep shine purple crystals were air dried to yield 2.2 g (20 % yield) of H_2TPP.[1] UV-vis (CH_2Cl_2) λ_{max}/nm: 420 (Soret), 448, 515, 552, 595, 648, as shown in Figure 5.

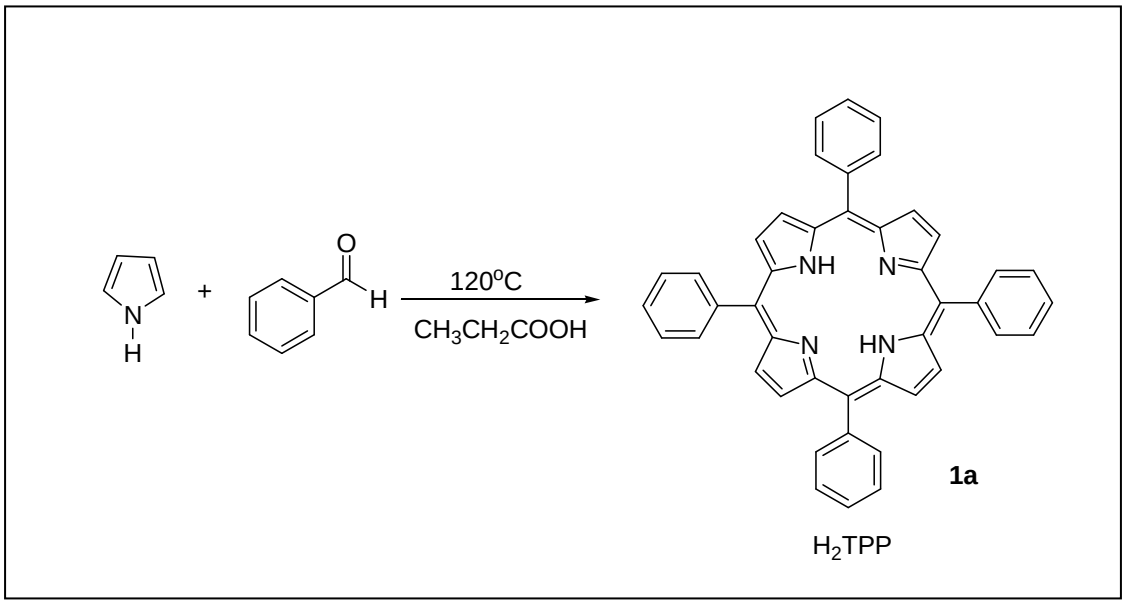

Scheme 7. Synthesis of H_2TPP **(1a)**

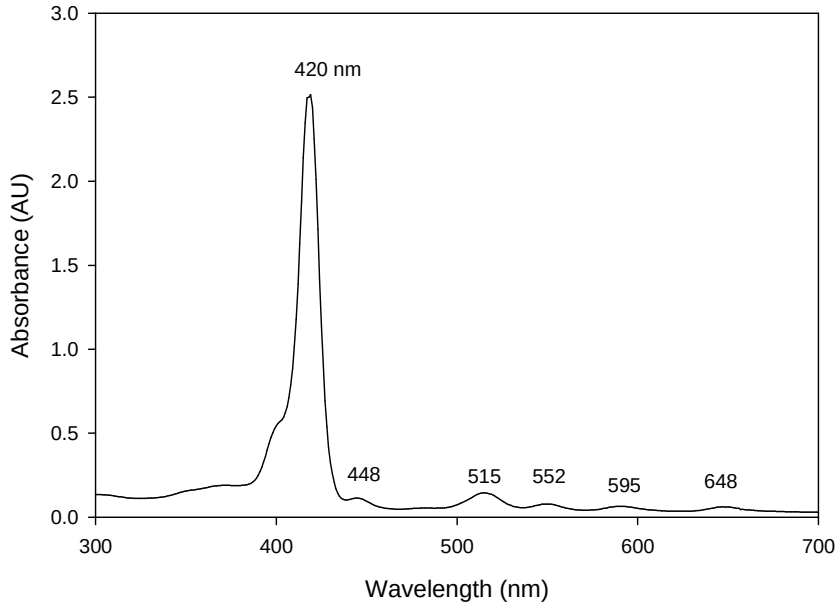

Figure 5. UV-vis spectrum of H_2TPP in CH_2Cl_2

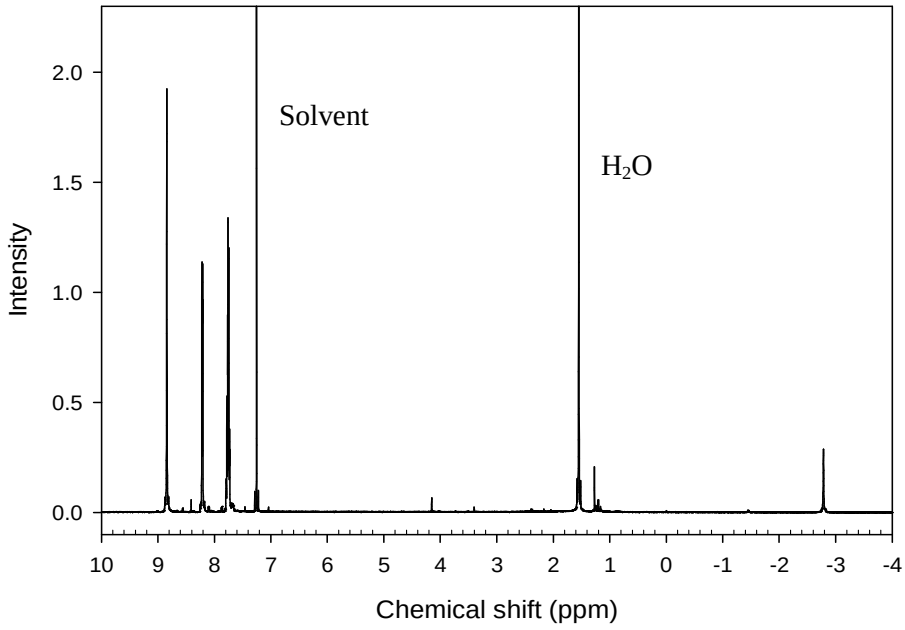

Figure 6. ^{1}H-NMR spectrum of H_2TPP

2.3.2. Synthesis and Characterization of Carbonyl Ruthenium(II) Porphyrin Complexes **(2)**

The carbonyl ruthenium(II) porphyrin complexes were synthesized according to the literature procedure developed by Che and co-workers (Scheme 8-9).[26] The reaction is solvent and temperature dependent. For the carbonyl (5, 10, 15, 20-tetraphenyl porphyrinato)-ruthenium(II) abbreviated as [Ru^{II}(CO)TPP] (**2a)**, decalin, a non-polar solvent, was used to provide a refluxing temperature at 180^{o}C. However, 1,2,4-trichlorobenzene which is a more polar solvent than decalin, was used for the synthesis of the more electron deficient complex, carbonyl (5,10,15,20-tetrapentafluorophenyl porphyrinato)-ruthenium(II) abbreviated as [Ru^{II}(CO)TPFPP] (**2b)**. The use of the more polar 1,2,4-trichlorobenzene at a higher temperature (220^{o}C) in the synthesis of **2b** resulted in a better yield compared to the use of the non-polar decalin (~ 10 % yield). Also, the synthesis of **2b** in 1,2,4-trichlorobenzene resulted in a much higher yield (93%) than earlier procedures using *o*-dichlorobenzene (55% yield).[27]

2.3.2.1. Preparation of Carbonyl (5,10,15,20-tetraphenylporphyrinato) Ruthenium(II) [Ru^{II}(CO)TPP] **(2a)**

A mixture of [$Ru_3(CO)_{12}$] (100 mg) and **1a** (100 mg) in 50 mL decalin (decahydronaphthalene) was refluxed and stirred for an hour and half (1.5 hr) at a temperature of about 180^{o}C (Scheme 8). The mixture was cooled to room temperature and an alumina column chromatography was used for product purification. An excess

amount of hexane was first used to remove all decalin. Dichloromethane was then used to remove any remaining free ligands. A mixture of acetone and dichloromethane (1:1 v/v) was used to elute the desired product, **2a**. The solvent was evaporated by rotary evaporation and a brick-red solid was obtained (90 % yield).

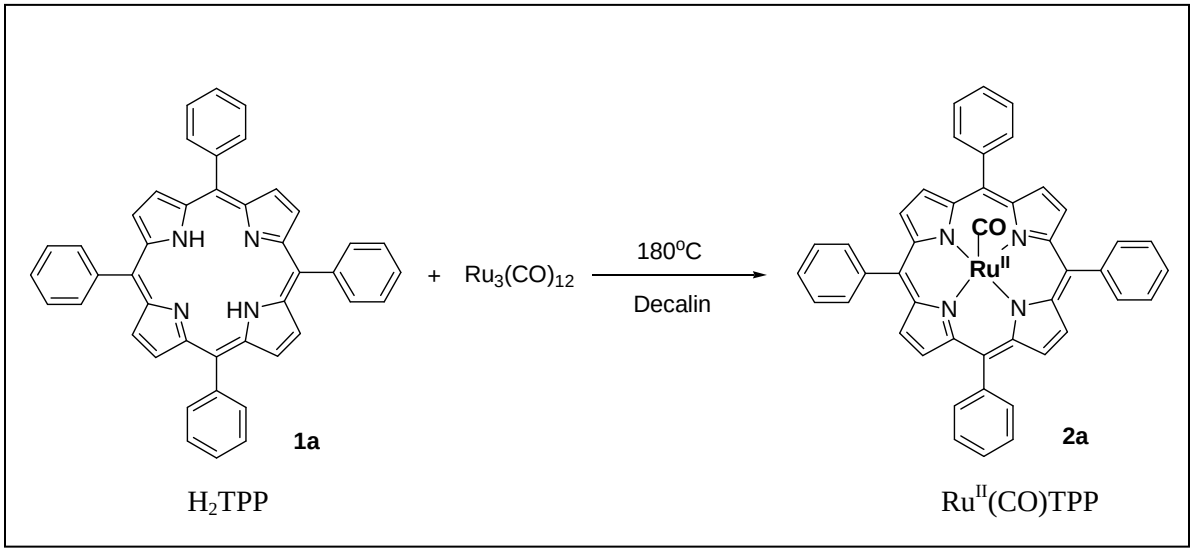

Scheme 8. Synthesis of $Ru^{II}(CO)TPP$ **(2a)**

The UV-vis spectrum of [$Ru^{II}(CO)TPP$] in dichloromethane (CH_2Cl_2) (Figure 7) shows a strong signal at 411 nm, which is known as the Soret band and a less intense signal at 532 nm, referred to as the Q band. ^1H NMR ($CDCl_3$): δ 8.68 (d, pyrrolic H, 8H), 7.46 (s, ArH, 4H) (Figure 8). IR (KBr, cm^{-1}): 1942, 1918 (ν_{CO}), 1010 (oxidation state marker band) (Figure 9).

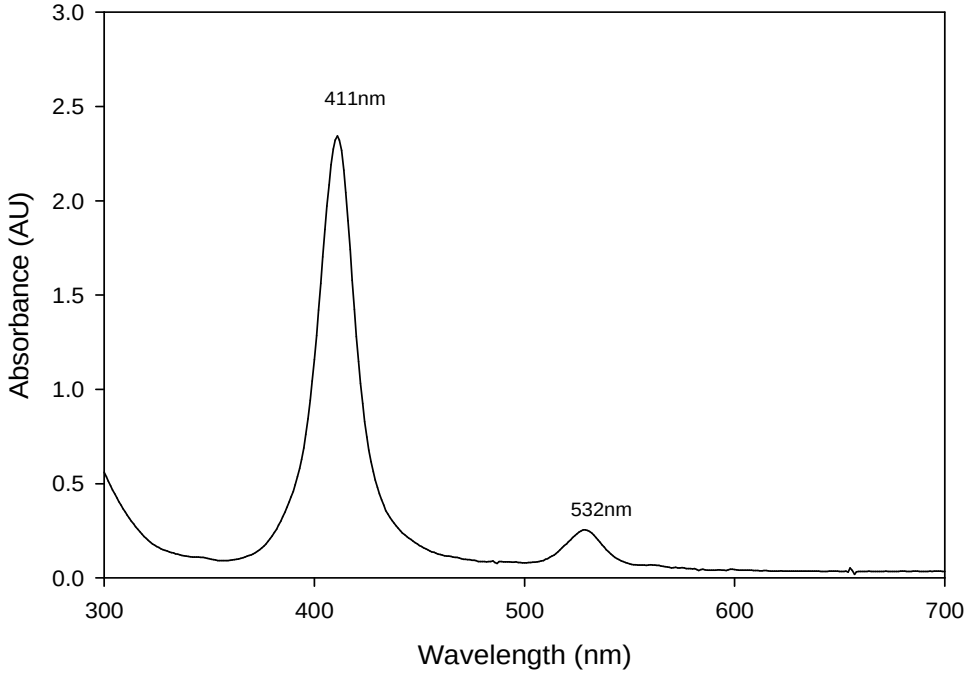

Figure 7. UV-vis spectrum of [Ru^{II}(CO)TPP] in CH_2Cl_2

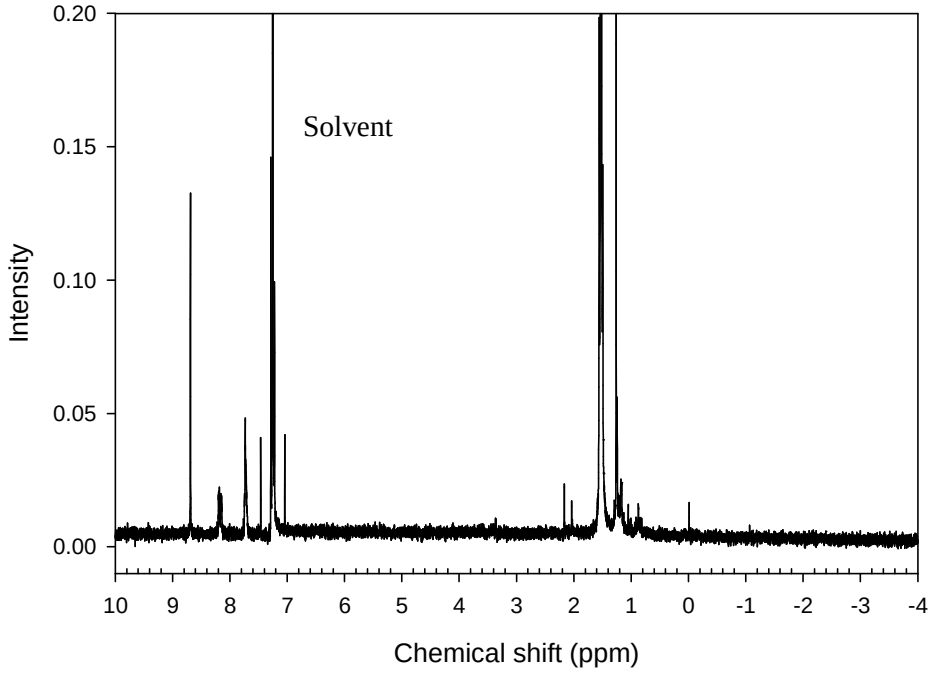

Figure 8. ^{1}H-NMR spectrum of [Ru^{II}(CO)TPP]

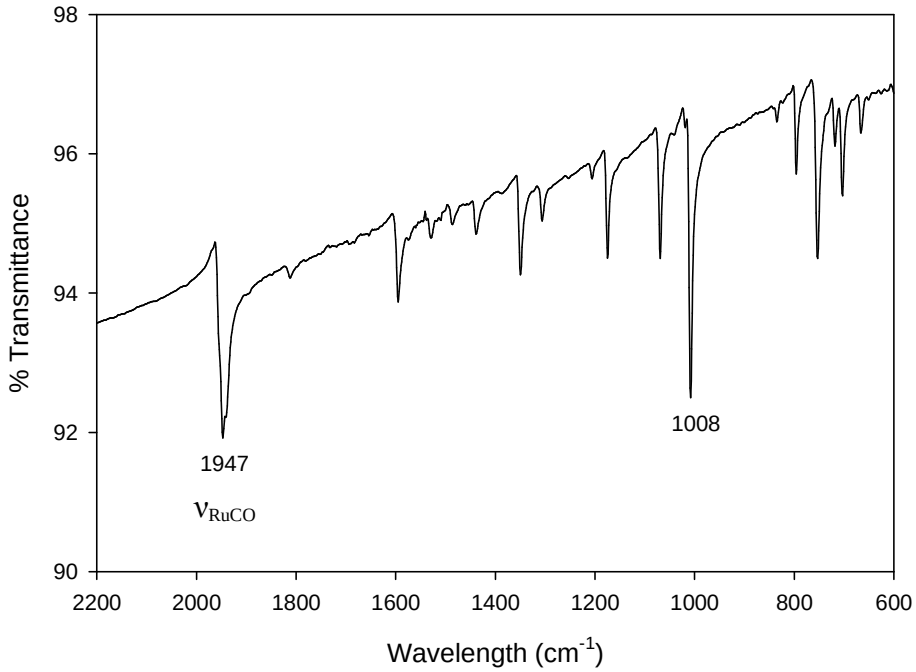

Figure 9. IR Spectrum of [Ru^{II}(CO)TPP] **2a** (KBr)

2.3.2.2 Preparation of Carbonyl (5,10,15,20-tetrakis(pentafluorophenyl)porphyrinato) Ruthenium(II) [Ru^{II}(CO)TPFPP] **(2b)**

A mixture of [$Ru_3(CO)_{12}$] (100 mg) and **1b** (100 mg) in freshly distilled 1,2,4-trichlorobenzene (50 mL) was refluxed overnight under argon (Scheme 9). The solvent of the mixture was then removed under vacuum, and the residue obtained was chromatographed on alumina column. A mixture of dichloromethane and hexane (1:1 v/v) was used to elute the unreacted free ligand and impurities. The brick red band containing the desired product was then eluted with a mixture of dichloromethane and acetone (1:1 v/v). The crude product was recrystallized from a CH_2Cl_2/n-hexane mixture

to give a dark purple solid product. The resulting crystals were air dried to yield 93 % of product, **2b**.

The UV-vis spectrum of [Ru^{II}(CO)TPFPP] in chloroform (Figure 10) shows a strong signal at 404 nm for the Soret band and a weak signal at 524 nm for the Q band. ^{1}H NMR ($CDCl_3$): δ 8.76 (pyrrolic H, 8H) (Figure 11). IR (KBr, cm^{-1}): 1958 (ν_{CO}), 1012 (oxidation state marker band) (Figure 12).

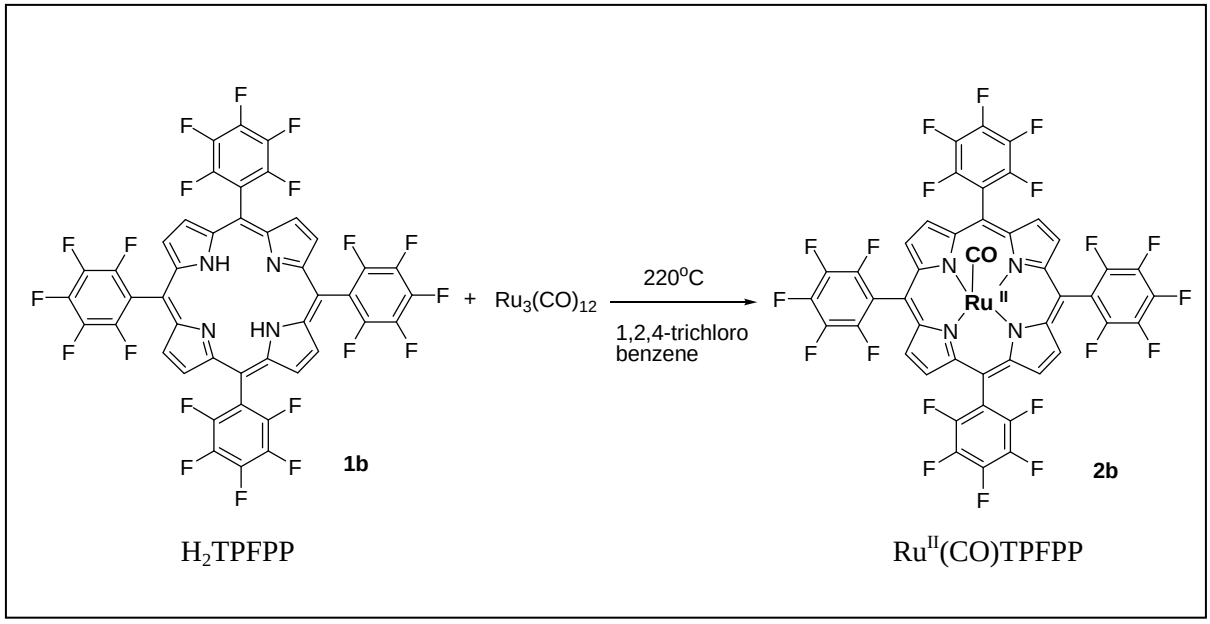

Scheme 9. Synthesis of [Ru^{II}(CO)TPFPP] **(2b)**

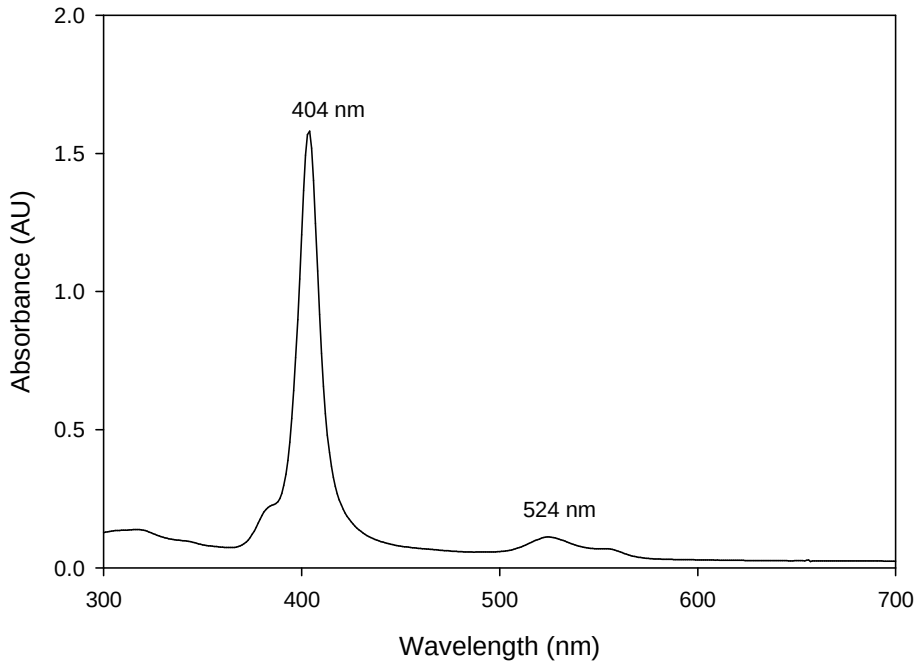

Figure 10. UV-vis spectrum of [Ru^{II}(CO)TPFPP] in $CHCl_3$

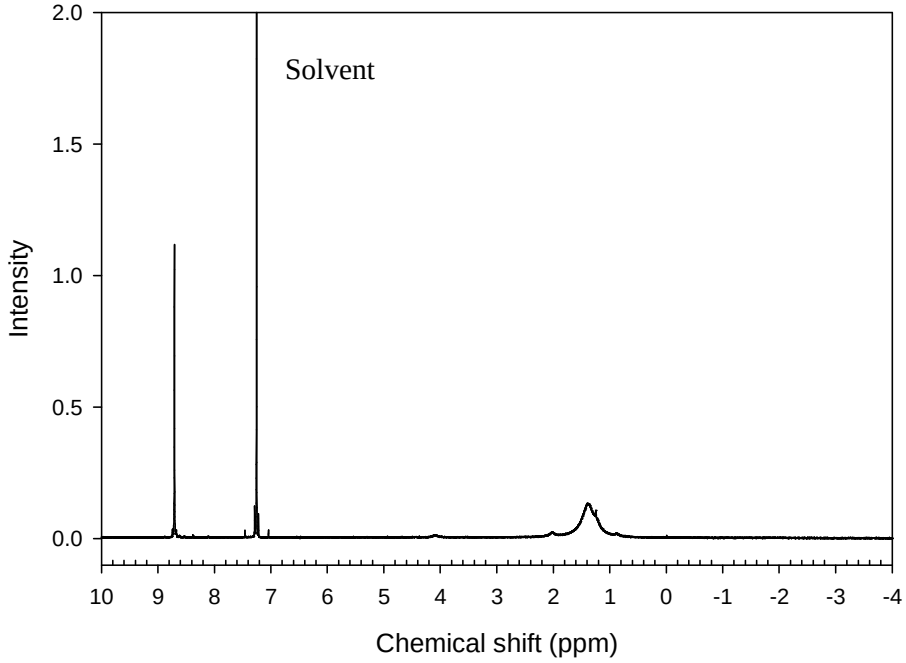

Figure 11. ^{1}H-NMR spectrum of Ru^{II}(CO)TPFPP

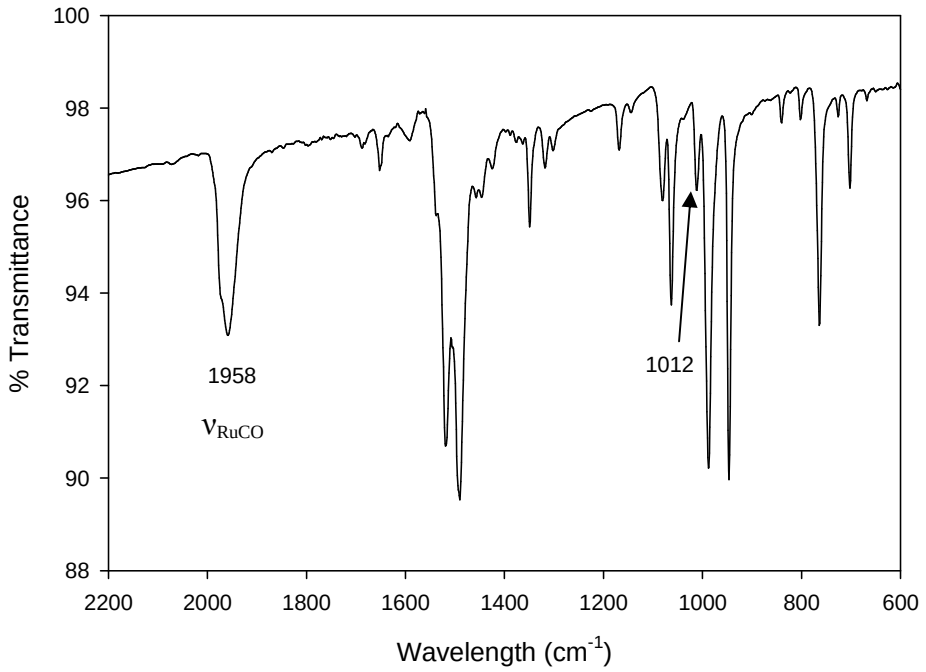

Figure 12. IR Spectrum of [Ru^{II}(CO)TPFPP] **3a** (KBr)

2.3.3 Synthesis and Characterization of *trans*-Dioxoruthenium(VI) Porphyrin Complexes **(3)**

2.3.3.1 Preparation of *trans*-Dioxo(5,10,15,20-tetraphenylporphyrinato) Ruthenium(VI) [$Ru^{VI}(O)_2$TPP] **(3a)**

The non-sterically hindered *trans*-dioxoruthenium(VI) porphyrin [$Ru^{VI}(O)_2$TPP] was synthesized from the oxidation of corresponding [Ru^{II}(CO)TPP] (**2a**) by *meta*-chloroperoxybenzoic acid (*m*-CPBA) in protic ethanol solvent according to known procedures reported by Che and co-workers.[19] Solid [Ru^{II}(TPP)(CO)] (100 mg) was

added to an ethanolic solution of largely excess *m*-CPBA (800 mg) (Scheme 10). The resulting mixture was stirred for about one hour. The purple solid formed was filtered and washed with ethanol until the filtrate was colorless.

The reaction yielded approximately 70 % of [$Ru^{VI}(O_2)$TPP] (**3a)**. The completion of the reaction was indicated by the disappearance of *v*(C=O) stretch at 1945 cm^{-1} and the appearance of a new O=Ru=O stretch at 819 cm^{-1} in the IR spectrum of the filtered solid.[19] UV-vis ($CHCl_3$) λ_{max}/nm: 418 (Soret band), 520 (Q band) (Figure 13). ^{1}H NMR ($CDCl_3$): δ 9.1 (s, pyrrolic H, 8H), 8.58 (s, ArH, 4H) (Figure 14). IR (KBr, cm^{-1}): 1017 (oxidation state marker band) and 819 ($\nu_{Ru=O}$) (Figure 15).

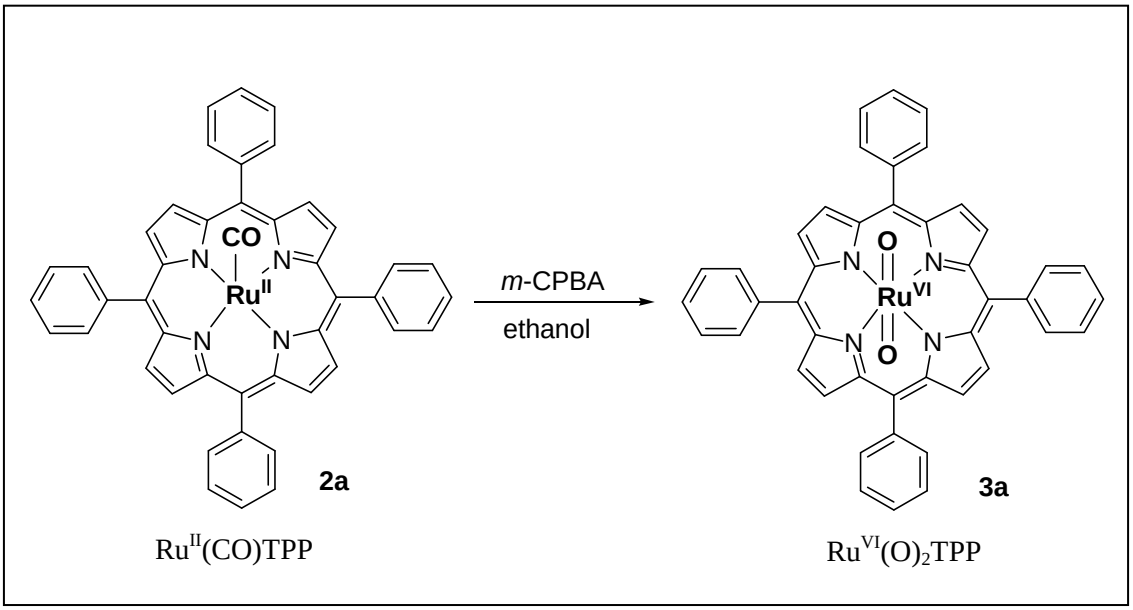

Scheme 10. Synthesis of [$Ru^{VI}(O)_2$TPP] **(3a)**

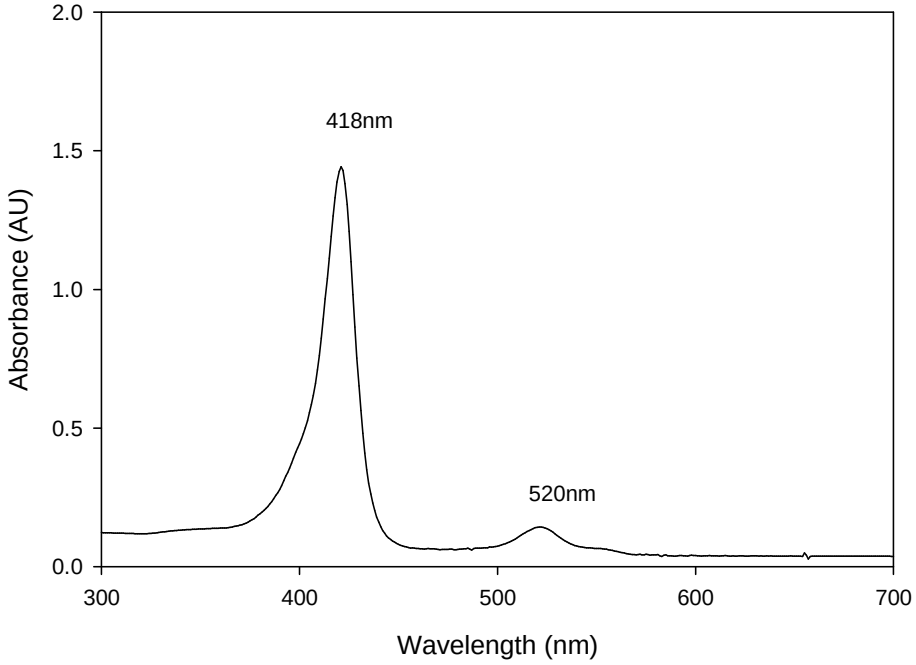

Figure 11. UV-vis of [$Ru^{VI}(O_2)$TPP] in $CHCl_3$

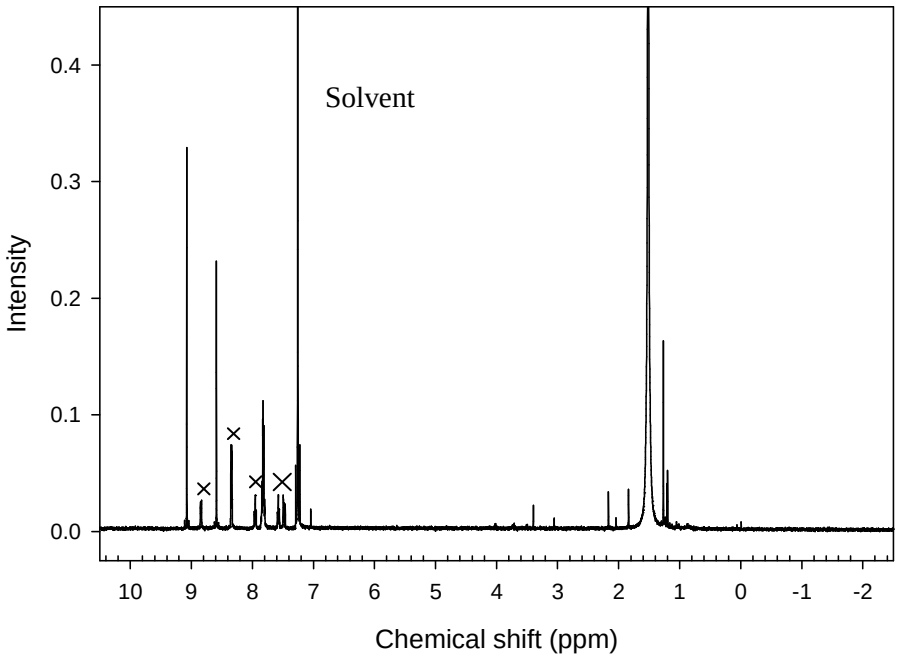

Figure 14. ^{1}H-NMR spectrum of $Ru^{VI}(O)_2$TPP

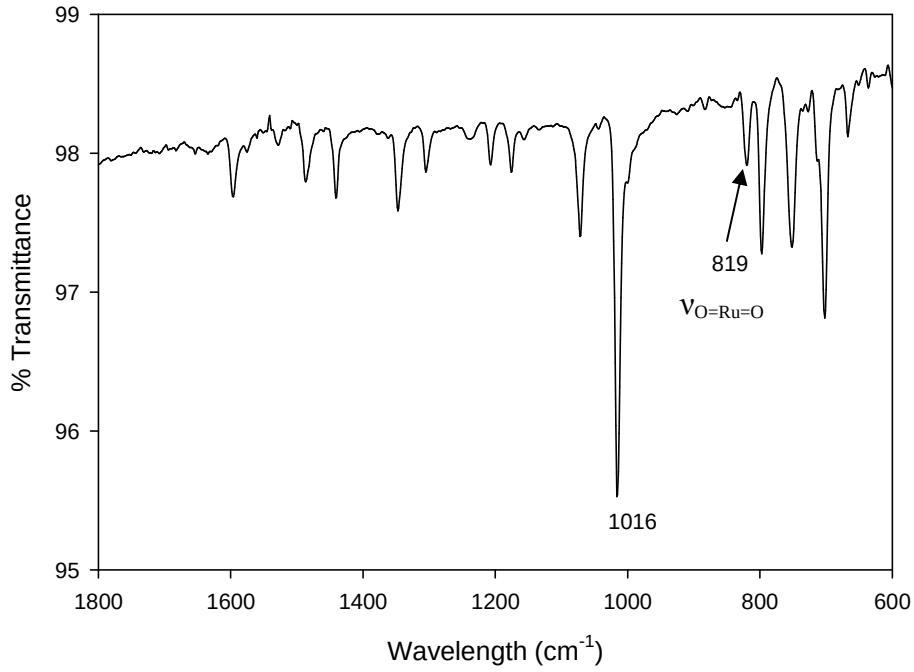

Figure 15. IR spectrum of $[Ru^{VI}(O)_2TPP]$ **3a** (KBr)

2.3.3.2 Preparation of *trans*-Dioxo(5,10,15,20-tetrakis(pentafluorophenyl) porphyrinato) Ruthenium (VI) $[Ru^{VI}(O)_2TPFPP]$ **(3b)**

The synthesis of sterically hindered $[Ru^{VI}(O)_2TPFPP]$ (**3b**) was based on the literature procedure reported by Groves et al.[18] This complex was mostly prepared on a micro-scale and used right afterwards. A chloroform solution of **2b** (2 mg) was treated with *m*-CPBA at room temperature (Scheme 11). The resultant mixture was swirled for about 1 minute, and was subjected to chromatography on a short alumina column. The dark brown product, **3b,** was eluted with $CHCl_3$.A yield of 90% was recorded. UV-vis (CH_2Cl_2): λ_{max}/nm = 412 (Soret band), 506 (Q band) as illustrated in Figure 16. ^{1}H NMR

($CDCl_3$): δ 9.18 (s, 8H; β-H), 8.53 (s, ArH, 4H) (Figure 17). IR (KBr, cm^{-1}): 1022 (oxidation state marker band) and 826 ($\nu_{Ru=O}$) (Figure 18).

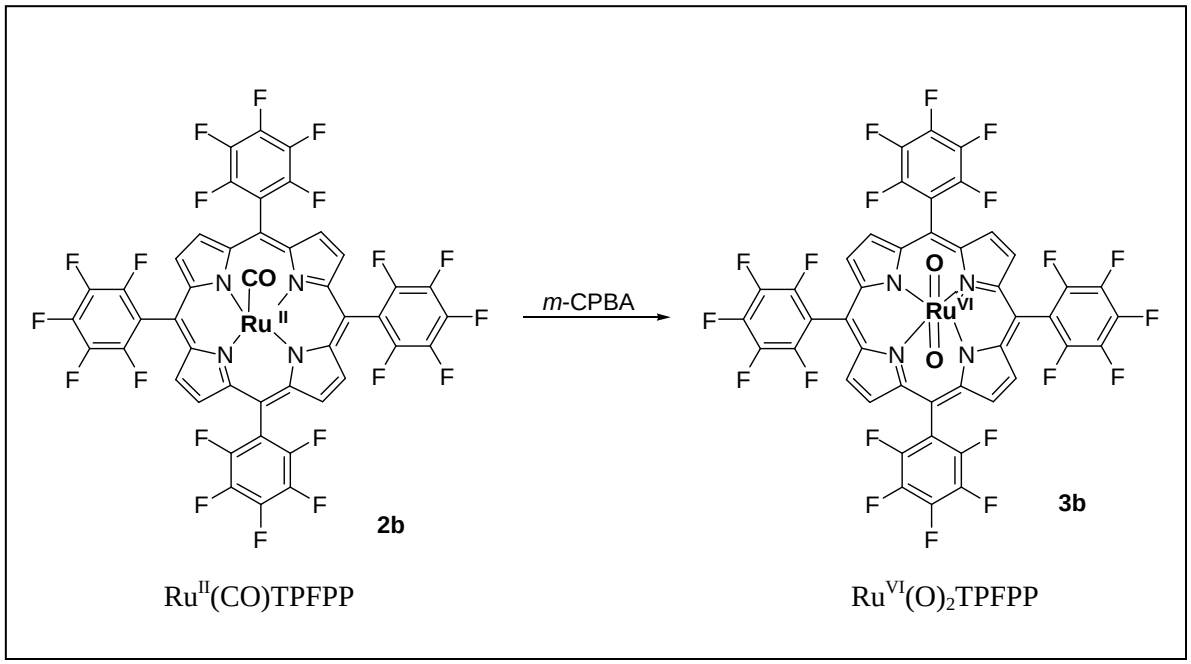

Scheme 11. Synthesis of [$Ru^{VI}(O)_2$TPFPP] **(3b)**

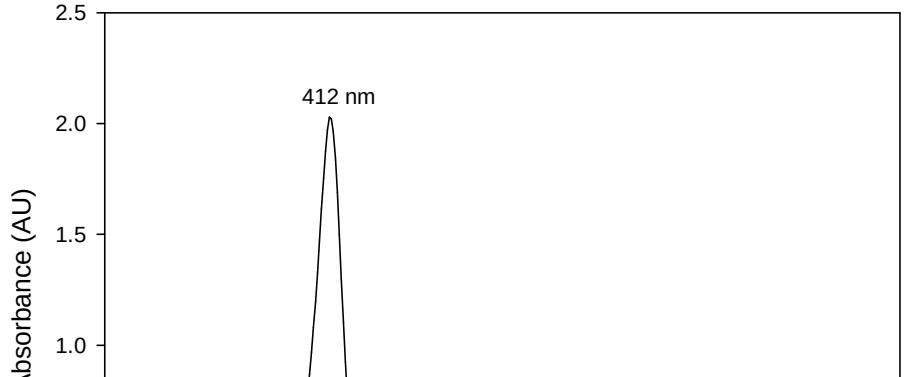

Figure 16. UV-vis spectrum of [$Ru^{VI}(O)_2$TPFPP] in CH_2Cl_2

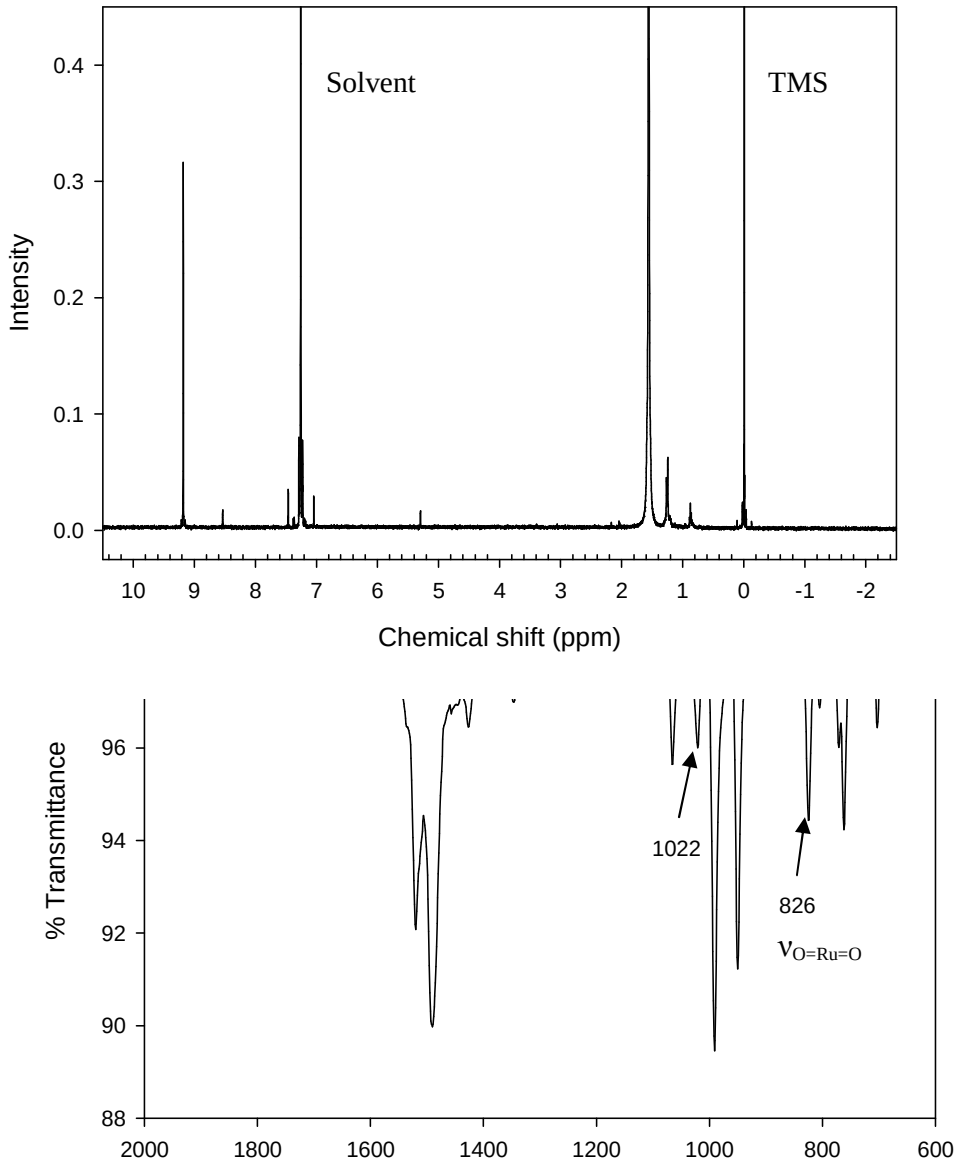

III. RESULTS AND DISCUSSION

3.1. Synthesis

The synthesis of the free ligands and the various ruthenium porphyrin complexes are well established in the literature.[5,18,19,25,27] As reported by Adler et al., the yield and rate of the condensation of pyrrole and benzaldehyde to H_2TPP (**1a**) depends on a number of factors such as the acidity, the solvent, the temperature, the availability of atmospheric oxygen, and the initial reagent concentration.[25] As a result, although, a 20 % yield of **1a** might not represent the highest yield, the reported procedure (Scheme 7) represents the most convenient method for rapidly and reproducibly obtaining a 20 ± 3 % yield of crystalline H_2TPP of relatively high purity.[25]

The metallation of the porphyrins occurred readily as reported. Treatment of $[Ru_3(CO)_{12}]$ with the free-base porphyrins (**1a**-**b**) in an inert solvent resulted in the insertion of ruthenium metal into the porphyrin ligands to yield the corresponding ruthenium(II) carbonyl complexes. The choice of the solvent is very important to the success of the synthesis.[19] In the preparation of $[Ru^{II}(CO)TPP]$ (**2a**), high-boiling decalin, as solvent, is effective with high yield (90 %). However, with the same solvent (decalin) the synthesis of $[Ru^{II}(CO)TPFPP]$ (**2b**) afforded less than 20 % of yield. Accordingly, 1,2,4-trichlorobenzene was found to be the choice of solvent for the synthesis of **2b** with a higher yield (93 %).[26] Also, the synthesis of **2b** in 1,2,4-trichlorobenzene resulted in a much higher yield (93 %) than earlier procedures using *o*-dichlorobenzene (55 % yield).[27]

The synthesis of the *trans*-dioxoruthenium(VI) porphyrins was effectively performed based on known procedures.[19,26,27] The oxidation of the sterically encumbered carbonyl ruthenium complex, **2b**, by *m*-CPBA yielded the corresponding *trans*-dioxoruthenium complex, **3b**. An ethanolic solution of *m*-CPBA was used for the preparation of the non-sterically hindered **3a**,[19] because its coordinating ability to ruthenium metal can avoid the undesired dimerization process. The *trans*-dioxoruthenium complexes are known to be relatively stable metal-oxo intermediates, which can be stored at -20^{o}C for months.[26] They are also low-reactive intermediates which makes them suitable for the kinetic studies. In this regard, *trans*-dioxoruthenium(VI) porphyrins are a promising class of oxidants for mechanistic investigation of organic oxidations by metal-oxo species.

3.2. UV-visible Spectra of the Ruthenium Porphyrins

The UV-visible spectral data of the ruthenium porphyrins are summarized in Table 1, and the actual spectra are illustrated in Figures 5, 7, 10, 13, and 16. The values obtained are consistent with literature values.[5,19,26,27] The UV-vis spectra of **2a-b** and **3a-b** are featured mainly by a strong Soret band, due to $\pi - \pi^*$ electron transfer, and a less intense Q band, as a result of n-π^* interaction. The spectrum of **1a** shows a strong signal for the Soret band and several less intense signals for the Q band which is typical of a normal free-base porphyrin ligand.[5]

Also notable on the UV-vis spectra is the fact that the Soret bands of the carbonyl ruthenium complexes (**2a-b**) are blue-shifted compared with the positions of absorption band of the corresponding *trans*-dioxoruthenium complexes (**3a-b**). However, the Q bands are red-shifted.

Table 1. UV-vis Spectral Data of Ruthenium Porphyrin Complexes in $CH_2Cl_2/CHCl_3$ at Room Temperature

	λ_{max} /nm	
Compound	Soret bands	Q bands
1a	420	448, 515, 552, 595, 648
1b	413	506, 584, 656
2a	411	532
2b	404	524
3a	418	520
3b	412	508

3.3. ^{1}H-NMR Spectra of the Ruthenium Porphyrins

The ruthenium porphyrin complexes (**2a-b, 3a-b**) were also characterized using ^{1}H-NMR as reported in the literature. Table 2 summarizes the results. The analysis of the data obtained is consistent with a compound with a diamagnetic electronic ground state,[5] d^6 for ruthenium(II) and d^2 for ruthenium(VI) complexes, respectively. As reported in the literature, the signals of the pyrrolic protons are known to be sensitive to the electron density of the porphyrin which is in turn affected by the ruthenium oxidation state.[5] The ^{1}H-NMR spectrum of the *trans*-dioxoruthenium complexes (**3a-b**) (Figure 14, 17) show the signal of the pyrrolic protons of the porphyrin ligands at 9.10 - 9.18 ppm, which is downfield from that of the carbonyl ruthenium complexes (**2a-b**) (Figure 8, 11) which is at 8.68 - 8.76 ppm as reported by Che et al.[26] The pyrrolic protons of **3a-b** appear as a pair of doublets compared to the singlets observed for **2a-b**. The change of the multiplicity in the conversion from Ru^{II} to Ru^{VI} is because the oxidation process is a symmetry ascending process.[5]

Table 2. ^{1}H Chemical Shifts (ppm) of the Ruthenium Porphyrin Complexes in $CDCl_3$

	Chemical shifts, δ ppm	
Compound	Pyrrolic H	Aryl H
2a	d, 8.68	s, 7.46
2b	d, 8.76	s, 7.35
3a	s, 9.10	s, 8.58
3b	s, 9.18	s, 8.53

3.4. Infrared Spectroscopy of the Ruthenium Porphyrins

FT-IR spectrometer was also used to characterize the ruthenium porphyrin complexes in accordance to literature. The IR spectra of **2a-b** and **3a-b** are shown in Figures 9, 12, 15, and 18, which are consistent with similar ruthenium porphyrin derivatives. The spectra show a strong and sharp absorption band around 1000 cm^{-1} which is assigned as the rocking vibration of the porphyrin ring or the pyrrole units.[5] As reported in the literature, this band is referred to as the oxidation state marker because of its sensitivity to the ruthenium oxidation state.[5] The oxidation state marker band lies in the range of 1007 - 1012 cm^{-1} for the carbonyl ruthenium(II) complexes (**2a-b**) (Figures 9, 12), and that for the *trans*-dioxoruthenium(VI) complexes (**3a-b**) (Figures 15, 18) are in the range of 1016 - 1022 cm^{-1}.The characteristic IR absorption peaks of the ruthenium porphyrins are listed in Table 3.

The *trans*-dioxoruthenium(VI) complexes show an intense band at 819 cm^{-1} for **3a** and at 826 cm^{-1} for **3b**, which are assigned as the O=Ru=O stretches. The oxidation of the metal center is also evidenced by the position of the oxidation marker, which has shifted from 1008 cm^{-1} in **2a** to 1016 cm^{-1} in **3a**,[19] and also from 1012 cm^{-1} in **2b** to 1022 cm^{-1} in **3b**. This signifies that the starting carbonyl complexes have been completely consumed.[5]

Table 3. Selected IR Absorption Peaks of Ruthenium Porphyrin Complexes

Compound	Peak position / cm^{-1}		
	Oxidation marker band $\nu_{(pyrrolic\ C-H)}$	$\nu_{C=O}$	$\nu_{as(O=Ru=O)}$
2a	1008	1947	
2b	1012	1958	
3a	1016		819
3b	1022		826

3.5. Kinetic Studies of the Ruthenium Porphyrin Complexes

Kinetic studies were conducted as detailed earlier in Section 2.2.4. In the presence of a large excess substrate, the active ruthenium(VI)-oxo porphyrin complex decayed with pseudo-first order kinetics to form Ru(IV) species. The pseudo-first order rate constants, k_{obs} , were determined by monitoring the disappearance of the Soret band of the *trans*-dioxoruthenium(VI) porphyrins in chloroform. Figure 19 depicts the representative UV-vis spectral change for the sulfide oxidation by the *trans*-dioxoruthenium(VI) porphyrin complex in chloroform. The isosbestic spectral change from Ru^{VI} to Ru^{IV} porphyrin indicates no intermediates accumulated during the process. This transformation is manifested by the decay of the Soret band of the *trans*-dioxoruthenium(VI) complex at 412 nm (λ_{max}) accompanied by the development of a new absorption[5] at 420 nm (λ_{max}), which is red-shifted in the sulfoxidation kinetics.

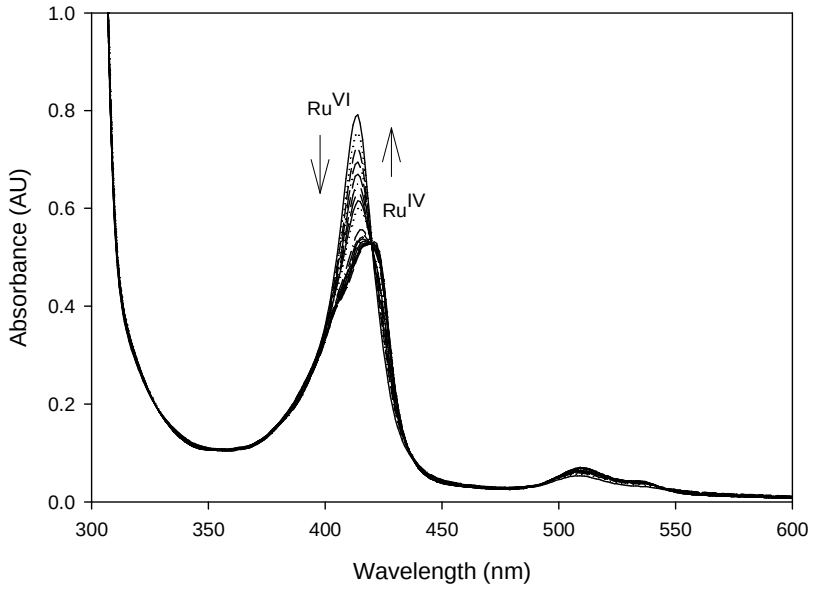

Figure 19. Time-resolved spectrum for the reaction of **3b** with phenyl methyl sulfide (0.125 mM) in $CHCl_3$ over 400 seconds.

Scheme 12 illustrates the stoichiometric oxidation of thioanisole by different *trans*-dioxoruthenium(VI) complexes as described in Section 2.2.3. The reaction yielded sulfoxide as the only detectable organic product without over-oxidation to sulfones. Product analysis was determined by the ^{1}H NMR spectrum which gave a signal at δ = 2.7 ppm due to the methyl group of sulfoxides. Based on the amount and type of the *trans*-dioxoruthenium(VI) complex, the yields of the sulfoxide ranged from 136 to 200 %, indicating a two two-electron oxo-transfer processes (Scheme 4.1). Also, monitoring the reaction by UV-vis spectroscopy showed the two processes involved (Figure 20). Its noteworthy that the kinetics conducted in this work focused on the first rapid oxo-transfer process.

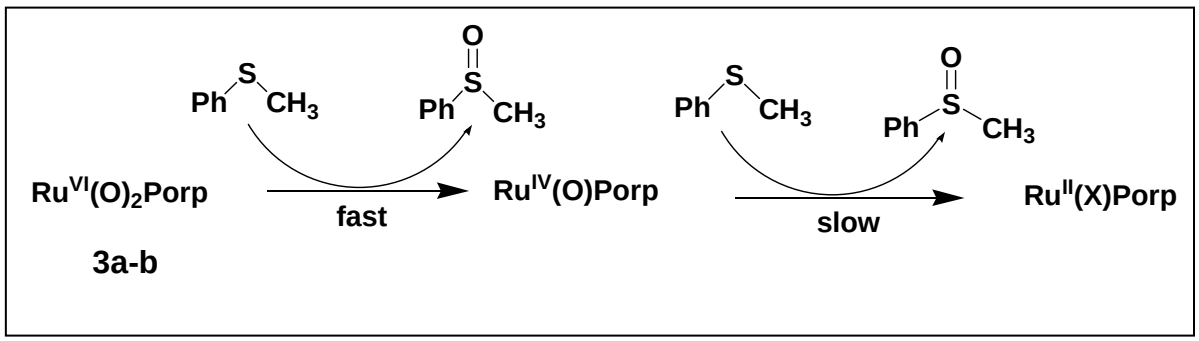

Scheme 12. Stoichiometric sulfoxidation by *trans*-dioxoruthenium(VI) complexes

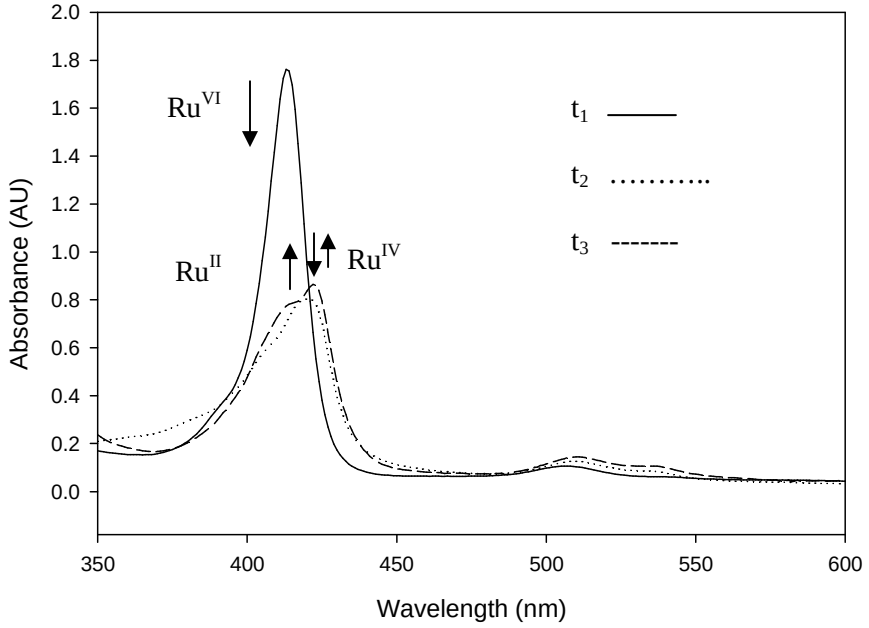

Figure 20. UV-vis spectrum of the reaction of **3b** with thioanisole in $CHCl_3$ showing two two-electron oxo-transfer processes monitored at times t_1= 0 min, t_2 = 1 min, and t_3 = 12 hrs

The kinetic studies of the sulfides oxidation reactions were conducted at four different concentrations of sulfides as shown by the kinetic traces (Figure 21). As shown in Figure 21, the kinetics of the sulfoxidation of the *trans*-dioxoruthenium(VI) porphyrin follows an exponential decay over four half-lives, and the rate of decay is dependent on the concentration of the substrates. Thus, the higher the concentration the higher the rate, and vice versa.

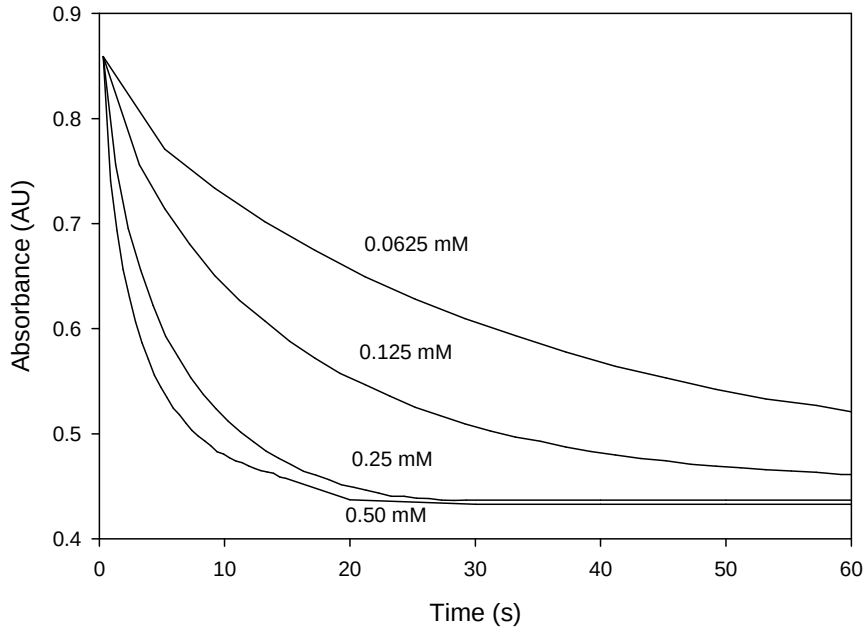

Figure 21. Kinetic traces monitored at 412 nm for the reaction of **3b** with thioanisole at varied concentrations in $CHCl_3$

The second-order rate constants were determined as the slope of the linear plot of the k_{obs} values versus substrate concentration according to the following equation:

$$k_{obs} = k_0 + k_2[\text{Sub}]$$

where k_{obs} is the observed pseudo-first order rate constant, k_0 is the background first-order rate constant for decay in the absence of substrate, k_2 is the second-order rate constant, and [Sub] is the molar concentration of the substrate.[16] Plots of k_{obs} versus [Sub] typically gave straight lines with near-zero intercepts as shown in Figure 22. The second-order rate constants for the reaction of the various ruthenium porphyrin complexes and a variety of substrates are summarized in Table 4.

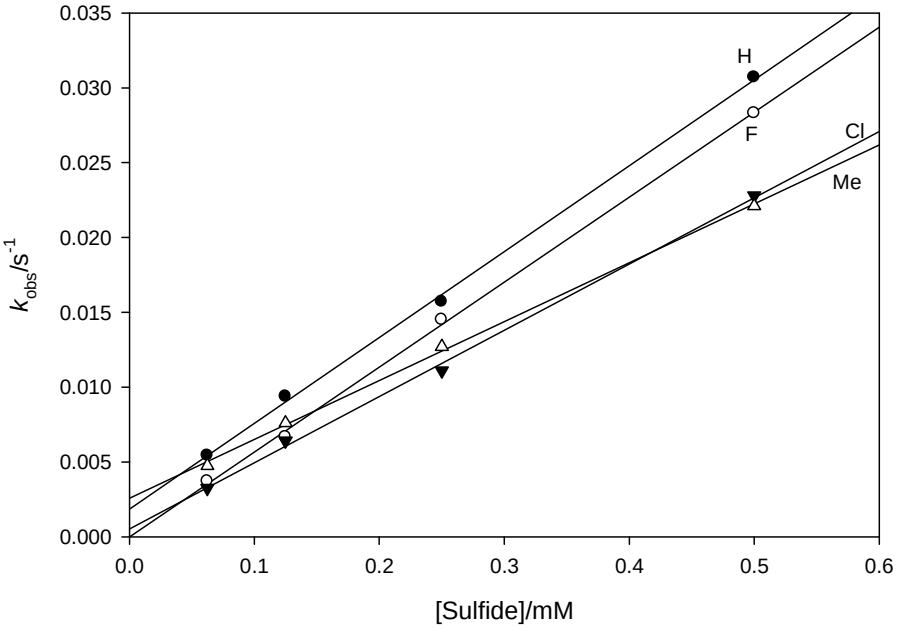

Figure 22. Observed rate constants for the reaction of **3b** with different substrates; thioanisole (H), *p*-fluorothioanisole (F), *p*-chlorothioanisole (Cl), and *p*-methylthioanisole (Me)

In a report by Chellamani et al. on the kinetics of sulfides catalyzed by a manganese-salen complex, it was stated that the sulfur atom of the sulfides is more positively charged in the transition state than it is in the reactant.[24] Thus, it is suggested that some amount of positive charge develop on the sulfide in the sulfoxidation mechanism of this process, influencing the reactivity of the various substrates based on their electronegativity. However, as shown on Figure 22, the effect of substituents on substrate for the oxidation of *para*-substituted aryl methyl sulfides was minor, implying that no appreciable charge developed on the sulfur during the oxidation process. This deduction was based on the fact that their k_2 values are not significantly different from each other (Table 4).

Chellamani et al. also conducted a study on the substituent effect of the oxidation of several *para*-substituted phenyl methyl sulfides based on the kinetic sulfoxidation by (salen)Mn^{III} complexes.[24] They reported that electron-donating substituents accelerate the rate, while electron-withdrawing substituents retard it,[24] due to the electrophilic nature of the metal center of the porphyrin complex. However, this effect was not observed because both the electron donating and withdrawing substituents showed slightly decelerating effects, as seen on Figure 22 and Table 4.

3.5.1. Comparison of the Reactivity of the Ruthenium Porphyrin Complexes

With available kinetic results, the reactivity of three *trans*-dioxoruthenium(VI) porphyrin complexes in different organic systems were also compared. Table 4 also shows the reactivity of the ruthenium(VI)-oxo species with thioanisole in the order **3b** > **3a** > **3c**, which is in accordance with the general observation that more highly electrophilic metal-oxo complexes, by virtue of the electron-withdrawing aryl groups, are more reactive oxidants. Also included in Table 4 for the purpose of comparison are the sulfoxidation kinetic data of $[Ru^{VI}(O)_2TMP]$, **3c** (Scheme 13).

As illustrated in Table 4, complex **3b** is the most reactive with the phenyl methyl sulfides, followed by complex **3a**, and then **3c**. This trend is consistent with the electrophilic nature of high-valent metal-oxo species. Complex **3b** is the most reactive due to the high electronegative effect of the fluorine atom substituents of the aryl groups

attached at positions 5, 10, 15, and 20, also known as the *meso*- position, of the porphyrin complex (Scheme 13).

Table 4. Second-Order Rate Constants (k_2) for the Reactions of a Variety of Substrates by Ruthenium Porphyrin Complexes in $CHCl_3$ at 22 ± 2°C.

Metal-oxo Species	Substrate	k_2 ($M^{-1}s^{-1}$)
$[Ru^{VI}(O)_2TPFPP]$	**thioanisole**	**59.6 ± 2.0**
3b	*p*-fluorothioanisole	56.0 ± 1.0
	p-chlorothioanisole	42.4 ± 3.0
	p-methylthioanisole	39.4 ± 2.0
	p-methoxythioanisole	38.0 ± 4.0
$[Ru^{VI}(O)_2TPP]$	**thioanisole**	**48.0 ± 2.0**
3a	*p*-chlorothioanisole	38.0 ± 3.0
$[Ru^{VI}(O)_2TMP]$	**thioanisole**	**8.00 ± 0.4**
3c	p-fluorothioanisole	3.00 ± 0.3
	p-chlorothioanisole	8.10 ± 0.5

The fluorine substituents of **3b** increase the electrophilicity of the ruthenium porphyrin complex. As reported by Che et al., halogenation makes the reactive intermediate more electrophilic by reducing the electron density of the porphyrin ring, thus promoting its reactivity.[26] In addition, halogenation of the porphyrin ligand enhanced the catalyst stability toward hydrocarbon oxidations as compared to their non-halogenated counterparts,[26] showing greater efficiency in catalyzing hydrocarbon oxidations.

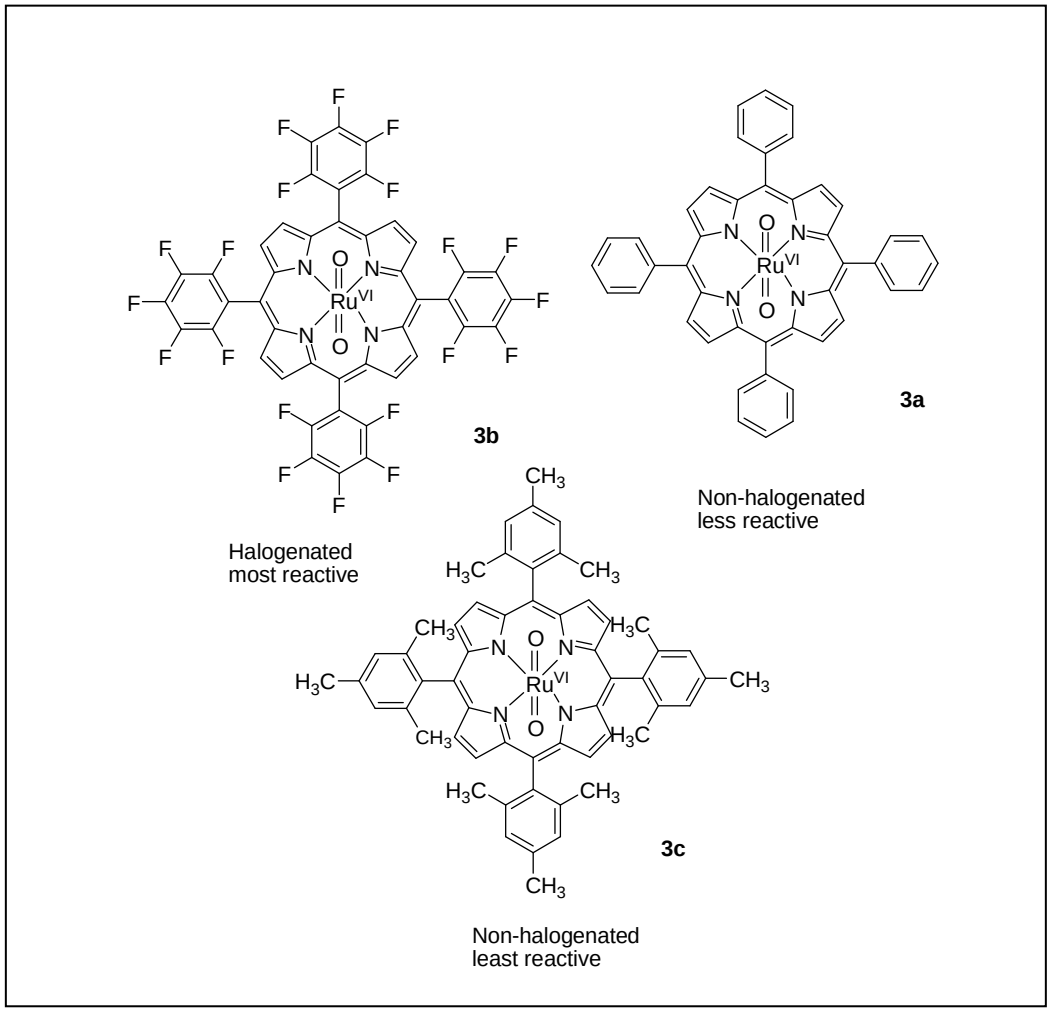

Scheme 13. Structures of the *trans*-dioxoruthenium(VI) porphyrin complexes relating halogenation and reactivity

Complex **3c** is the least reactive because of the steric effect of methyl substituents of the aryl groups at the *meso*- positions of the porphyrin. The methyl groups form a fence around the complex blocking the substrate from interacting with the complex thereby reducing the reactivity.

3.5.2. Comparison of Sulfoxidation and Epoxidation Kinetic Studies

Studies on the epoxidation of hydrocarbons by high-valent metal-oxo species to yield the corresponding epoxides are well documented. The discovery of metalloporphyrin complexes as suitable catalyst for hydrocarbon epoxidation has generated intensive interest in this field. There have been several papers reported on the kinetic studies of epoxidation of alkenes in the past decades. Zhang et al. described the catalytic enatioselective oxidation of aromatic hydrocarbons with D_4-symmetric chiral ruthenium porphyrin catalysts.[17] Che et al. also reported on the hydrocarbon oxidation by β-halogenated dioxoruthenium(VI) porphyrin complexes.[2] However, the kinetic studies of oxidation of sulfides to corresponding sulfoxides and sulfones are still sparse in literature. Chellamani and co-workers published a paper on the kinetics and mechanism of (salen)Mn^{III}-catalysed hydrogen peroxide oxidation of alkyl aryl sulphides.[24] There is still no available kinetic data on the sulfoxidation of phenyl methyl sulfides by *trans*-dioxoruthenium porphyrin complexes. To date, the mechanism of sulfoxidation reactions is still less understood.

The kinetic data on epoxidation and sulfoxidation by complex **3b** brought forth some notable differences. First and foremost, the UV-vis spectral changes depict some differences in the transformation process. The spectral change for *cis*-cyclooctene oxidation by **3b** shows the decay of the Soret band of **3b** at 412 nm (λ_{max}) and the development of a new absorption band at 406 nm (λ_{max}) which is blue-shifted (Figure 23), whereas that of thioanisole is red-shifted (Figure 19). This signifies that the two reaction processes are different with possible different mechanism pathways.

However, both spectra indicate the transformation from Ru^{VI} to Ru^{IV} without any intermediate accumulation. The use of pyrazole in the epoxidation kinetic was essential for obtaining an isosbestic spectral change.[5] According to the known literature, pyrazole spontaneously reacts with the putative Ru(IV)-oxo intermediates to form $[Ru^{IV}(Por)(pz)_2]$ without accumulation of intermediates.[5]

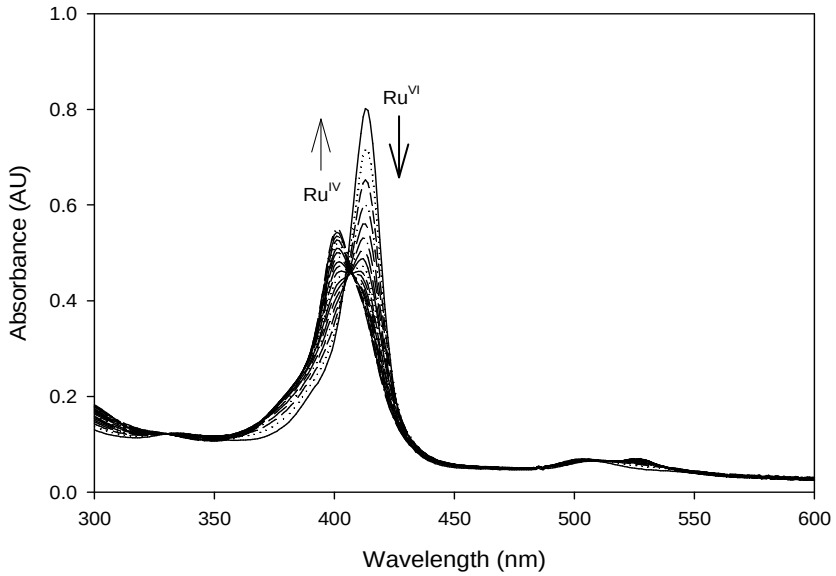

Figure 23. UV-vis spectral changes during the reaction of complex **3b** with *cis*-cyclooctene (0.125 M) in chloroform with 2% w/w pyrazole over 1200 seconds

Figures 21 and 24 depict the kinetic traces for the sulfoxidation and epoxidation reactions at different concentrations. Although the overall positive charge developing on the sulfur in the oxidation process is minimal, it can be suggested that it is more pronounced in the sulfoxidation kinetics than in the epoxidation kinetics. Notably, the sulfoxidation kinetic was favorable at a much lower concentration (millimolar) of substrate and shorter time (Figure 21) compared to the epoxidation kinetic which was conducted at a higher concentration of substrate and longer time (Figure 24). Thus, the kinetic results clearly show that the sulfoxidation reaction is much faster than the epoxidation reaction under similar conditions.

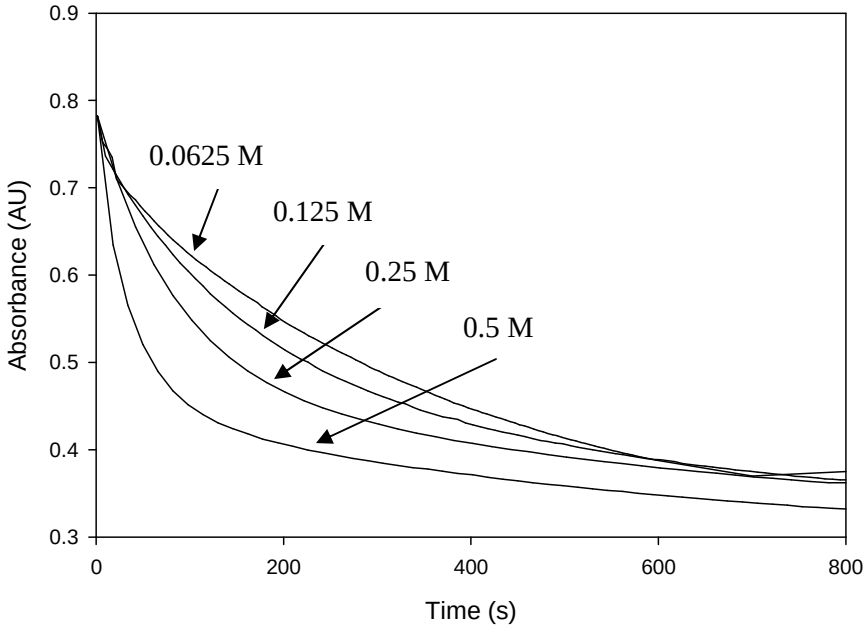

Figure 24. Kinetic traces monitored at 412 nm for the reaction of **3b** with *cis*-cyclooctene at varied concentrations

Consequently, the second-order rate constants for the sulfoxidation and epoxidation kinetic studies ascertained that the sulfoxidation reaction is faster than the epoxidation reaction in this study. The kinetic plot of k_{obs} versus thioanisole at different concentrations produced a second-order rate constant (slope) of 59.6 $M^{-1}s^{-1}$ compared to 25.7 x 10^{-3} $M^{-1}s^{-1}$ obtained as the slope from the kinetic plot of the reaction with *cis*-cyclooctene at varied concentrations (Figures 25-26). In view of this, it can be deduced from this study that sulfoxidation with **3b** is 3 – 4 orders of magnitude faster than epoxidation with **3b** under similar conditions. Figures 25 and 26 show the kinetic plots of the sulfoxidation and epoxidation kinetic studies depicting a linearly increase of rate with substrate concentrations, indicating that the kinetics of the two oxidation processes are concentration dependent.

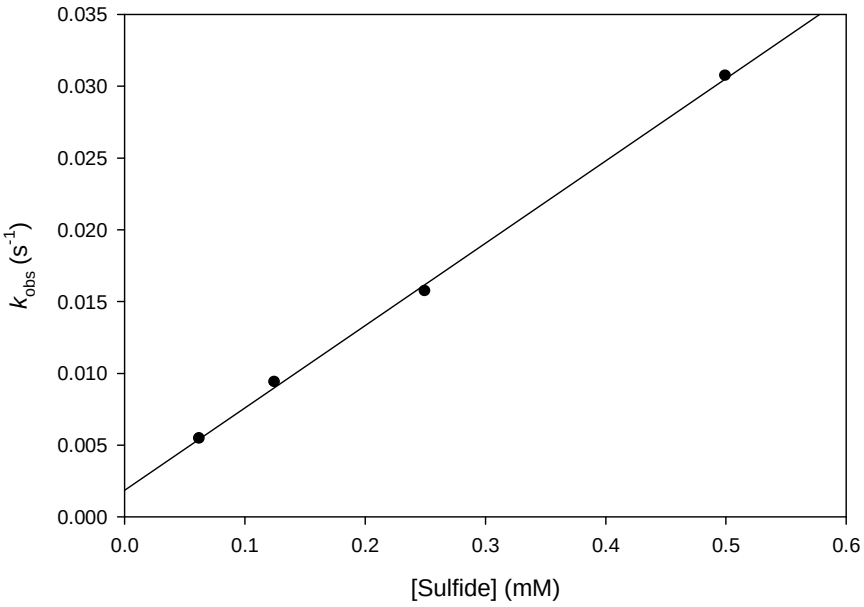

Figure 25. Kinetic plot of the reaction of 3b with thioanisole at 0.5 mM, 0.25 mM, 0.125 mM, and 0.0625 mM. (k_2 = 59.6 $M^{-1}s^{-1}$, R = 0.9989)

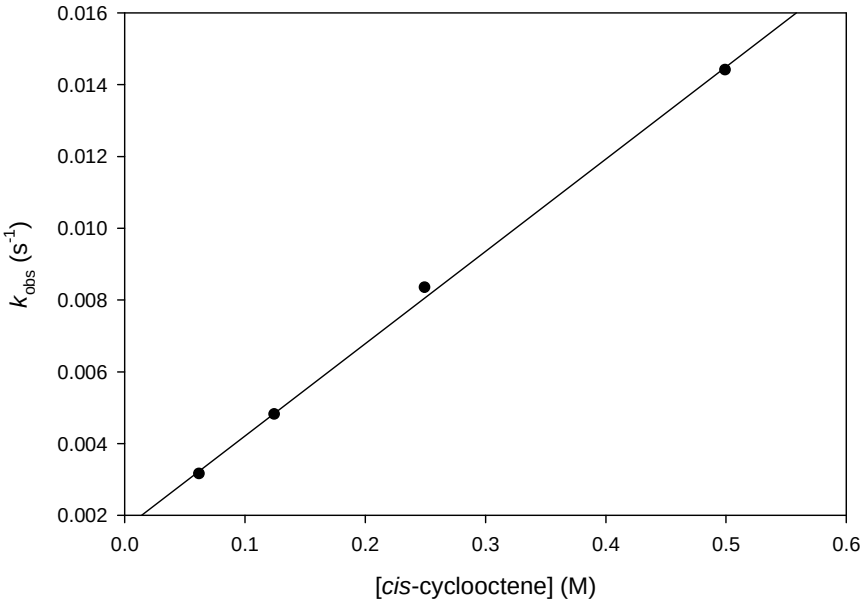

Figure 26. Kinetic plot of the reaction of **3b** with *cis*-cyclooctene at 0.5 M, 0.25 M, 0.125 M, and 0.0625 M. (k_2 = 25.7 x 10^{-3} $M^{-1}s^{-1}$, R = 0.9987)

IV. CONCLUSION

A variety of ruthenium porphyrin complexes have been synthesized and spectroscopically characterized in accordance with literature knowledge. Metallation of the free ligands (**1a-b**) yielded the corresponding carbonyl ruthenium(II) porphyrin complexes (**2a-b**), which were isolated as pure solids. The choice of solvent is very important in this synthesis, since the synthesis of complex **2a** was more successful and efficient, in terms of yield (90%), in decalin (a non-polar solvent), whereas the synthesis of complex **2b** was most efficient in the more polar 1,2,4-trichlorobenzene (93% yield). The *trans*-dioxoruthenium(VI) porphyrin complexes (**3a-b**) were synthesized from the oxidation of their carbonylruthenium(II) porphyrin precursors with *m*-CPBA. The non-sterically hindered complex **3a** was isolated as a solid product in a coordinating medium. The sterically hindered complex **3b** was synthesized on a micro-scale in a non-coordination solvent and used immediately. The *trans*-dioxoruthenium(VI) porphyrin complexes are relatively stable and can be stored at -20^{o}C for months. They are also low-reactivity and promising oxidants for mechanistic investigation of sulfoxidation, a demanding task that has not been attempted yet. The spectroscopical data obtained for the UV-vis, ^{1}H-NMR, and IR spectra are all consistent with literature values.

A considerable number of kinetic studies of the oxidation of aryl methyl sulfides (Sulfoxidation) by *trans*-dioxoruthenium(VI) porphyrin complexes have been conducted. Product analysis by ^{1}H-NMR shows a selective oxidation of the sulfides to sulfoxides without over-oxidation to sulfones. Also, stiochiometric analysis of the product depicted two two-electron oxo-transfer processes; however, the kinetic studies were focused on the

first rapid oxo-transfer process. In the presence of a large excess substrate, the active ruthenium(VI)-oxo porphyrin complex decayed with pseudo-first order kinetics to form Ru(IV) species. The pseudo-first order rate constants increased linearly with substrate concentration, indicating that the kinetics of the oxidation process is concentration dependent. The time-resolved spectrum for the reaction of **3a-b** with the aryl methyl sulfides shows an isosbestic spectral change from Ru^{VI} to Ru^{IV} species, indicating no intermediates accumulated during the process.

The reactivity of the *trans*-dioxoruthenium(VI) species with thioanisole are in the order **3b** > **3a** > **3c**, which is in agreement with the general observation that more highly electrophilic metal-oxo complexes, by virtue of the electron withdrawing aryl groups, are more reactive oxidants. The reactivity of complex **3b** is enhanced by the more electronegative fluorine substituents of the aryl groups at the *meso*-positions of the porphyrin complex. Nonetheless, the effect of substituents on substrate for the oxidation of the *para*-substituted aryl methyl sulfides was minor, implying that no appreciable charge developed on the sulfur during the oxidation process.

The second-order rate constant for the sulfoxidation kinetic studies with **3b** was 59.6 $M^{-1}s^{-1}$ compared to 25.7 x 10^{-3} $M^{-1}s^{-1}$ obtained for the epoxidation kinetics, indicating that the sulfoxidation reaction with **3b** is 3 – 4 orders of magnitude faster than the epoxidation reaction with **3b** under similar conditions. Although, the mechanism for the sulfoxidation reaction is less understood, the kinetic results clearly shows that it does follow the same mechanism as the epoxidation reaction. Consequently, it can be deduced

from this study that *trans*-dioxoruthenium(VI) porphyrin complexes are proven selective oxidants for the oxidation of sulfides to the corresponding sulfoxides.

REFERENCES

1. Backwell, J.-E.; Piera J. Catalytic oxidation of organic substrates by molecular oxygen and hydrogen peroxide by multistep electron transfer – A biomimetic approach. *Angew. Chem. Int. Ed*. **2008**, *47*, 3506 – 3523.

2. ten Brink, G.-J.; Arends, I. W. C. E.; Sheldon, R. A. Green, catalytic oxidation of alcohols in water. *Science* **2000**, *287*, 1636 - 1639

3. Sheldon, R. A.; Arends, I. W. C. E.; ten Brink, G.-J.; Dijksman, A. Green, catalytic oxidation of alcohols. *Acc. Chem. Res*. **2002**, *35*, 774 – 781.

4. Groves, J.T.; Shallyaev, K.; Lee, J. *The Porphyrin Handbook* **2000**, *4*, 17 – 40.

5. Zhang, R. Asymmetric organic oxidation by chiral ruthenium complexes containing D_2 – and D_4 symmetric porphyrinato ligands. *Ph. D. Thesis* **2000**, 1 – 235.

6. Denisov, L.G.; Makris, M.T.; Sligar, G.S.; Schlichting, L. Structure and chemistry of cytochrome P450. *Chem. Rev*. **2005**, *105*, 2253 – 2277.

7. Newcomb, M.; Zhang, R.; Chandrasena, E. P.; Halgrimson, J. A.; Horner, J. H.; Makris, M. T.; Sligar, S. G. Cytochrome P450 Compound I. *J. Am.Chem. Soc*. **2006**, *128*, 4580 – 4581.

8. Masanori, S.; Roach, M. P.; Coulter, E. D.; Dawson, J. H. Heme – Containing Oxygenases. *Chem. Rev*. **1996**, *96*, 2841 – 2887.

9. Groves, J. T. Reactivity and mechanism of metalloporphyrin-catalyzed oxidations. *J. Porph. Phthal.* **2000**, *4*, 350 – 352.

10. Meunier, B. Metalloporphyrins as versatile catalyst for oxidation reactions and oxidative DNA cleavage. *Chem. Rev*. **1992**, *92*, 1411 – 1456.

11. Bernhardt, R.; Virus, C. Molecular evolution of a steroid hydroxylating cytochrome P450 using a versatile steroid detection system for screening. *Lipids* **2008**, *43*, 1133 – 1141.

12. Yano, J. K.; Koo, L. S.; Schuller, D. J.; Li, H.; Ortiz de Montellano, P. R. Crystal structure of a thermophilic cytochrome P450 from the archaeon *Sulfolobus solfataricus*. *J. Biol. Chem*. **2000**, *275*, 31086 – 31092.

13. Rui, L.; Pochapsky, S. S.; Pochapsky, C. T. Comparison of the complexes formed by cytochrome $P450_{cam}$ with cytochrome b_5 and putidaredoxin, two effectors of camphor hydroxylase activity. *Biochem*. **2006**, *45*, 3887 – 3897.

14. Poulos, T. L.; Finzel, B. C.; Gunsalus, I. C.; Wagner, G. C.; Kraut, J. The 2.6-Å crystal structure of pseudomonas putida cytochrome P450. *J. Biol. Chem*. **1985**, *260*, 16122 – 16130.

15. Hays, A.-M. A.; Dunn, A. R.; Chiu, R.; Gray, H. B.; Stout, C. D.; Goodin, D. B. Conformational states of cytochrome $P450_{cam}$ revealed by trapping of synthetic molecular wires. *J. Mol. Biol*. **2004**, *344*, 455 – 469.

16. Zhang, R.; Nagraj, N.; Lansakara-P., D. S. P.; Hager, L. P.; Newcomb, M. Kinetics of two-electron oxidation by the Compound I derivative of chloroperoxidase, a model for cytochrome P450 oxidants. *Org. Lett*. **2006**, *8*, 2731 – 2734.

17. Che, C.-M.; Zhang, R.; Yu, W.-Y. Catalytic enantioselective oxidation of aromatic hydrocarbons with D_4-symmetric chiral ruthenium porphyrin catalysts. *Tetrahedron: Asymmetry* **2005**, *16*, 3520 – 3526.

18. Wang, C.; Shalyaev, K. V.; Bonchio, M.; Carofiglio, T.; Groves, J. T. Fast catalytic hydroxylation of hydrocarbons with ruthenium porphyrins. *Inorg. Chem*. **2006**, *45*, 4769 – 4782.

19. Che, C.-M.; Leung, W.-H. High-Valent Ruthenium(IV) and –(VI) oxo complexes of octaethylporphyrin. Synthesis, spectroscopy, and reactivities. *J. Am. Chem. Soc*. **1989**, *111*, 8812 – 8818.

20. Kowalski, P.; Mitka, K.; Ossowska, K.; Kolarska, Z. Oxidation of sulfides to sulfoxides. Part1: Oxidation using halogens derivatives. *Tetrahedron* **2005**, *61*, 1933 – 1953.

21. Golchoubian, H.; Hosseinpoor, F. Mn(III)-catalyzed oxidation of sulfides to sulfoxides with hydrogen peroxide. *Tetrahedron Lett*. **2006**, *47*, 5195 – 5197.

22. Kaczorowska, K.; Kowalski, P.; Mitka, K.; Kolarska, Z. Oxidation of sulfides to sulfoxides. Part 2: Oxidation by hydrogen peroxide. *Tetrahedron* **2005**, *61*, 8315 – 8327.

23. Surendra, K.; Krishnaveni, N. S.; Kumar, V. P.; Sridhar, R.; Rao, K. R. Selective and efficient oxidation of sulfides to sulfoxides with *N*-bromosuccinimide in the presence of β-cyclodextrin in water. *Tetrahedron Lett*. **2005**, *46*, 4581 – 4583.

24. Chellamani, A; Alhaji, N.M. I.; Rajagopal, S. Kinetics and mechanism of (salen)MnIII – catalyzed hydrogen peroxide oxidation of alkyl aryl sulphides. *J. Phys. Org. Chem.* **2007**, *20*, 255 – 263.

25. Adler, A.D.; Longo, F.R.; Finarelli, J.D.; Goldmacher, J.; Assour, J.; Korsakoff, L. A Simplified synthesis for *meso*-Tetraphenylporphin. *J. Org. Chem*. **1966**, *32*, 476.

26. Che, C.-M.; Zhang, J.-L.; Zhang, R.; Huang, J.-S.; Lai, T.-S.; Tsui, W.-M, Zhou, X.-G.; Zhou, Z.-Y.; Zhu, N.; Chang, C. K. Hydrocarbon oxidation by β-halogenated dioxoruthenium(VI) porphyrin complexes: Effect of reduction potential (RuVI/V) and C – H bond-dissociation energy on rate constants. *Chem. Eur. J*. **2005**, *11*, 7040 – 7053.

27. Groves, J. T.; Bonchio, M.; Carofiglio, T.; Shalyaev, K. Rapid catalytic oxygenation of hydrocarbons by ruthenium pentafluorophenylporphyrin complexes: Evidence for the involvement of a Ru(II) intermediate. *J. Am. Chem. Soc*. **1996**, *118*, 8961 – 8962.